



Novel tacrine-coumarin hybrids linked to 1,2,3-triazole as anti-Alzheimer's compounds: *In vitro* and *in vivo* biological evaluation and docking study

Zahra Najafi^{a,b}, Mohammad Mahdavi^c, Mina Saeedi^{d,e}, Elahe Karimpour-Razkenari^e, Najmeh Edraki^f, Mohammad Sharifzadeh^g, Mahnaz Khanavi^h, Tahmineh Akbarzadeh^{a,e,*}

^a Department of Medicinal Chemistry, Faculty of Pharmacy, Tehran University of Medical Sciences, Tehran, Iran

^b Department of Medicinal Chemistry, School of Pharmacy, Hamadan University of Medical Sciences, Hamadan, Iran

^c Endocrinology and Metabolism Research Center, Endocrinology and Metabolism Clinical Sciences Institute, Tehran University of Medical Sciences, Tehran, Iran

^d Medicinal Plants Research Center, Faculty of Pharmacy, Tehran University of Medical Sciences, Tehran, Iran

^e Persian Medicine and Pharmacy Research Center, Tehran University of Medical Sciences, Tehran, Iran

^f Medicinal and Natural Products Chemistry Research Center, Shiraz University of Medical Sciences, Shiraz, Iran

^g Department of Pharmacology and Toxicology, Faculty of Pharmacy, Tehran University of Medical Sciences, Tehran, Iran

^h Department of Pharmacognosy, Faculty of Pharmacy, Tehran University of Medical Sciences, Tehran, Iran

ARTICLE INFO

This paper is dedicated to our wonderful teacher in chemistry and medicinal chemistry, Professor Abbas Shafiee (1937–2016).

Keywords:

Alzheimer's disease
Tacrine-Coumarins
1,2,3-Triazole
Docking study
Dual binding site
Morris water maze

ABSTRACT

A new series of tacrine-coumarin hybrids linked to 1,2,3-triazole were designed, synthesized, and tested as potent dual binding site cholinesterase inhibitors (ChEIs) for the treatment of Alzheimer's disease (AD). Among them, compound **8e** was the most potent anti-AChE derivative ($IC_{50} = 27$ nM) and compound **8m** displayed the best anti-BChE activity ($IC_{50} = 6$ nM) much more active than tacrine and donepezil as the reference drugs. Compound **8e** was also evaluated for its BACE1 inhibitory activity and neuroprotectivity against PC12 cells exposed to $A\beta_{25-35}$ which indicated low activity. Finally, *in vivo* studies by Morris water maze task showed that compound **8e** significantly reversed scopolamine-induced memory deficit in rats.

1. Introduction

Alzheimer's disease (AD) is a progressive neurodegenerative disorder and the most common form of dementia worldwide [1,2]. The cause of AD is still unclear and has been described by the several reasons such as genetic factors [3–5], amyloid- β peptides aggregation [6], neurofibrillary tangles (NFTs) [7], cholinergic hypofunction, oxidative stress [8], metal ion dyshomeostasis [9], and inflammation [10], etc. Among them, the cholinergic hypofunction has been known as one of the significant causes of AD [11]. Acetylcholine (ACh) plays an important role in attention, learning, memory and motivation. One of the main ways to increase ACh level in the brain is inhibition of cholinesterase enzymes (ChEs). There are two ChEs known as acetylcholinesterase (AChE) and butyrylcholinesterase (BChE) that catalyze the hydrolysis of ACh. In the healthy brain, AChE has predominant activity in terminating ACh-mediated neurotransmission whereas BChE acts as the secondary enzyme [12,13]. In patients with AD, a misbalance takes place between AChE and BChE so that the activity of

AChE does not change or decreases whereas BChE activity significantly increases. Therefore, it seems that both enzymes are involved in regulating of the ACh level and considered as valuable therapeutic targets against AD. As a result, dual inhibition of AChE and BChE enzymes would be more useful for AD patients in the late stages of disease than AChE selective inhibitors.

The crystal structural studies of both AChE and BChE enzymes revealed that they possess two binding sites including the catalytic site (CS) and peripheral anionic site (PAS) [14,15]. However, they have shown high binding affinity towards substrates and inhibitors. The main difference between them is associated with acyl binding site (ABS) in such a manner that of BChE is significantly bigger than of AChE. It seems that stimulatory inhibition of CS and PAS affords inhibitors that are more potent. In addition, recent evidences suggested that the PAS of AChE plays key roles in $A\beta$ -aggregation [16,17]. Also, BChE knockout animal model showed diminished fibrillar $A\beta$ plaque deposition suggesting that the lack of BChE reduces deposition of fibrillar $A\beta$ in AD [18]. Consequently, a great deal of attention has been paid to the

* Corresponding author at: Department of Medicinal Chemistry, Faculty of Pharmacy, Tehran University of Medical Sciences, Tehran, Iran.

E-mail address: akbarzad@tums.ac.ir (T. Akbarzadeh).

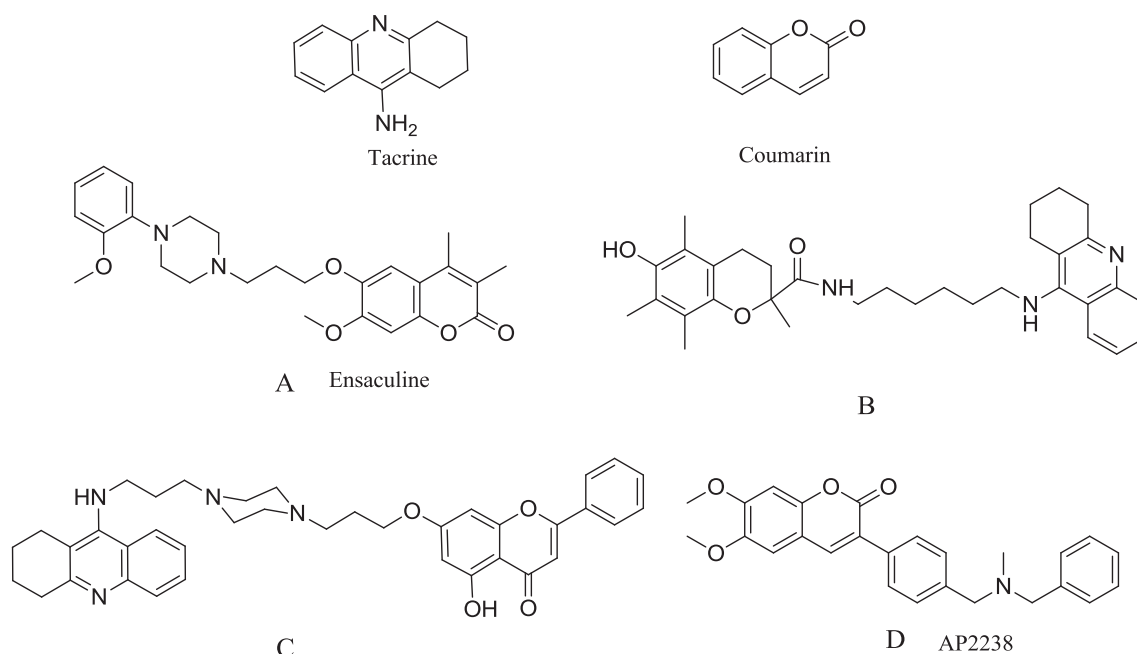


Fig. 1. Anti- AChE and BChE agents: tacrine and coumarin containing compounds.

development of dual AChE and BChE inhibitors to increase inhibitory activity *via* increasing the ligand-target interaction. According to the literature, tacrine has been found as a specific inhibitor of the catalytic anionic site (CAS) of CS whereas coumarin has affinity for the PAS of ChEs [19,20]. All structures demonstrated in Fig. 1(A–D) showed the importance of coumarin and tacrine scaffolds in the development of ChEIs [20–22].

Based on the above mentioned reports and in continuation of our work on the synthesis and evaluation of anti-Alzheimer's compounds [23,24], we designed and synthesized novel hybrid tacrine-coumarin-1,2,3-triazoles which prepared through click chemistry approach (Scheme 1). All compounds **8a-r** were evaluated for their *in vitro* and *in vivo* anti-Alzheimer's activity.

2. Results and discussion

2.1. Chemistry

The desired compounds **8a-r** were obtained by the reaction sequence illustrated in Scheme 1. The reaction of anthranilic acid derivatives **1a-c** and cyclohexanone **2** in refluxing POCl_3 for 3 h gave 1,2,3,4-tetrahydroacridine derivatives **3a-c** [25,26]. Compounds **3a-c** were treated with propargylamine in phenol at 100 °C for 2 h to afford propargylated acridine derivatives **4a-c** [27]. Further reaction series is associated with preparation of desired azide derivatives **7a-f**. For this purpose, coumarin **5a** was commercially obtained from Merck and 4-methyl-7-hydroxycoumarin (**5b**) was prepared by Pechmann reaction *via* the condensation of resorcinol and ethylacetoacetate in the presence of concentrated sulfuric acid [28]. Compounds **5a-b** were reacted with different dibromoalkanes in the presence of anhydrous potassium carbonate in acetonitrile at 80 °C for 4 h to give compounds **6a-f** [29–31]. Compounds **7a-f** [32,33] were obtained by the reaction of compounds **6a-f** with sodium azide in ethanol. After evaporation of solvent, the residue was used for the next step without purification. Finally, desired products **8a-r** were prepared by click reaction of compounds **4a-c** with azide derivatives **7a-f** in $\text{H}_2\text{O}/t\text{-BuOH}$ (1:1) in the presence of Et_3N along with a catalytic amount of CuI at room temperature for 12–24 h [23].

The structure of all synthesized compounds was confirmed using ^1H NMR and ^{13}C NMR spectroscopy. They were in good agreement with

those expected chemical shifts and coupling patterns. For example, ^1H NMR spectrum of compound **8e** showed eight protons belonging to four methylene groups of 1,2,3,4-tetrahydroacridine moiety around 1.86, 2.69, and 3.01 ppm as multiplet and triplet signals. The presence of methyl group and three methylene linker protons were confirmed by multiplet signal around 2.36–2.41 ppm and triplet signals at 3.98 and 4.54 ppm. Also, methylene group protons connected to NH was depicted as a singlet signal at 4.68 ppm. Singlet proton related to proton at 3-position of coumarin was observed at 6.13 ppm and accordingly H_5 , H_6 , and H_8 of coumarin moiety were observed at 7.47, 6.78, and 6.74 ppm as doublet, doublet of doublet, and doublet signals, respectively with desired coupling constants. The H_5 , H_7 , and H_8 of 1,2,3,4-tetrahydroacridine moiety were distinguished at 7.89, 7.27, and 7.90 ppm as singlet, doublet, and doublet signals, respectively. Finally, the existence of proton belonging to 1,2,3-triazole moiety was observed at 7.26 ppm as a singlet signal. Moreover, ^{13}C NMR spectrum confirmed nine aliphatic, nineteen aromatic, and a carbonyl group distinct resonances.

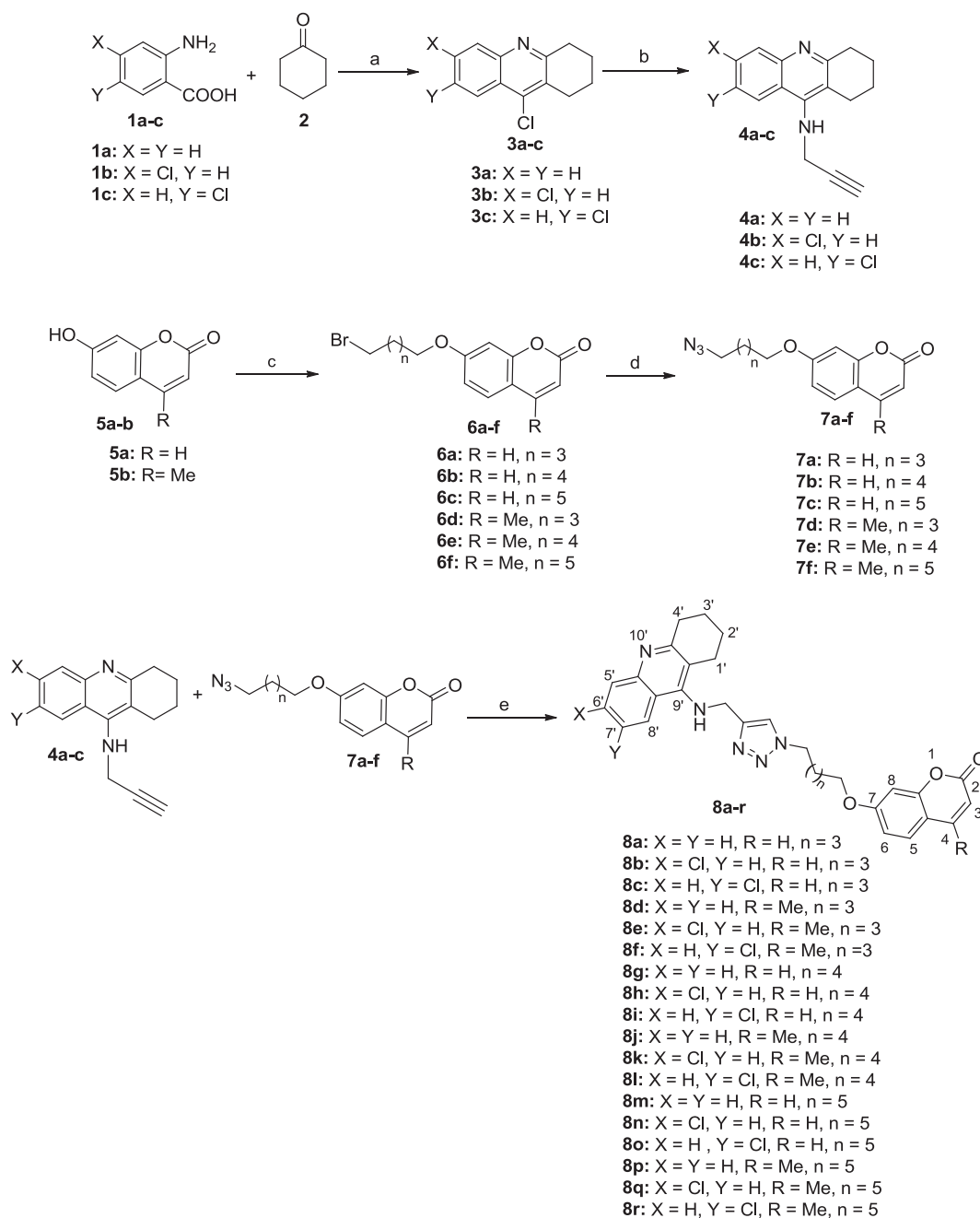
2.2. Pharmacology

2.2.1. AChE and BChE inhibitory activity

The *in vitro* AChE and BChE inhibitory activity of all synthesized compounds **8a-r** was evaluated using modified Ellman's method [34] and compared with tacrine and donepezil as the reference drugs (Table 1). All data were presented as the mean \pm SD of three independent experiments. Among the synthesized compounds **8a-r**, the most potent anti-AChE and anti-BChE activities were related to compounds **8e** ($\text{IC}_{50} = 0.027 \mu\text{M}$) and **8m** ($\text{IC}_{50} = 0.006 \mu\text{M}$), respectively.

In all designed compounds, 1,2,3,4-tetrahydroacridine and coumarin cores were connected by methylene groups and 1,2,3-triazole moiety. Synthesized compounds **8a-r** can be divided into three series based on the length of methylene linker: **8a-f**, **8g-l**, and **8m-r** possessing three, four and five methylene groups, respectively.

In the case of AChEI activity, compound **8e** belonging to the first series having Cl at 6-position of 1,2,3,4-tetrahydroacridine and methyl at 4-position of coumarin exhibited the best anti-AChE activity with IC_{50} value of 0.027 μM , more potent than tacrine and donepezil with IC_{50} value of 0.048 and 0.039 μM , respectively. Changing the position of Cl significantly decreased the anti-AChE activity in compound **8f**



Scheme 1. Synthesis of tacrine-coumarin hybrids **8**: (a) POCl₃, reflux, 3 h, 70–80%; (b) Propagylamine, PhOH, 100 °C, 2 h, 75%; (c) dibromoalkanes, K₂CO₃, acetonitrile, reflux, 3–4 h, 95%; (d) NaN₃, ethanol, reflux, 3–4 h, 95%; (e) CuI, H₂O/*t*-BuOH, NEt₃, 12–24 h, 48–68%.

(IC₅₀ = 1.674 μM), however deletion of Cl in compound **8d** led to the decrease of activity in comparison to compound **8f** in such a manner that the order of activity was **8e** > **8d** > **8f**. Considering the inhibitory activity of compounds **8a**, **8b**, and **8c** in the first series of compounds revealed that the presence of Cl at 6-position of tetrahydroacridine moiety plays important role as compound **8b** showed AChEI activity with IC₅₀ = 0.056 μM. Also, it was found that the presence of methyl group at 4-position of coumarin moiety is remarkable and similar order of activity was observed for **8b** > **8a** > **8c**. It was clear that the lack of methyl group in compounds **8a**, **8b**, and **8c** led to the decrease of activity comparing with their counterparts **8d**, **8e**, and **8f**.

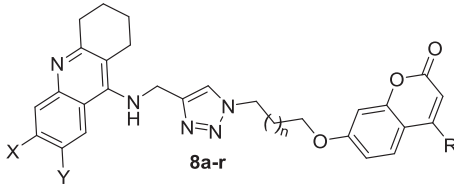
In the second series of synthesized compounds (**8g-l**) having linker with four methylene groups, compounds **8g**, **8h**, **8j**, and **8k** were found to be strong toward AChE since the following IC₅₀s = 0.046, 0.044,

0.066, and 0.068 μM were calculated, respectively. In this series of compounds, the presence of Cl at 6-position of tetrahydroacridine moiety as well as lack of Cl significantly affected anti-AChE activity. However, the presence of Cl at 7-position of tetrahydroacridine moiety deteriorated AChEI activity in compounds **8i** and **8l** (IC₅₀s = 1.829 and 0.614 μM). Also, the presence of methyl played no important role.

Considering our results obtained from the third series of compounds (**8m-r**) confirmed similar anti-AChE activity as observed for the first series (**8a-f**). As expected the presence of Cl at 6-position of tetrahydroacridine moiety and methyl at 4-position of coumarin increased AChEI activity since compounds **8m**, **8n**, and **8o** showed IC₅₀s = 0.095, 0.052, and 0.738 μM whereas their counterparts, compounds **8p**, **8q**, and **8r** showed IC₅₀s = 0.050, 0.039, and 0.273 μM, respectively.

To sum up, SAR studies showed that anti-AChE activity was completely affected by the absence and presence of Cl and Me groups as

Table 1
The IC₅₀ values of the compounds **8a-r** against AChE and BChE.^a



Entry	Compound 8	n	R	X	Y	AChEI [IC ₅₀ (μM)]	BChEI [IC ₅₀ (μM)]	Selectivity index AChE ^b BChE ^c	
1	8a	1	H	H	H	0.176 ± 0.007	0.032 ± 0.011	0.182	5.500
2	8b	1	H	Cl	H	0.056 ± 0.011	0.328 ± 0.027	5.857	0.171
3	8c	1	H	H	Cl	1.775 ± 0.024	≥10	–	–
4	8d	1	Me	H	H	0.474 ± 0.013	0.450 ± 0.008	0.949	1.053
5	8e	1	Me	Cl	H	0.027 ± 0.009	0.104 ± 0.018	3.852	0.260
6	8f	1	Me	H	Cl	1.674 ± 0.017	≥10	–	–
7	8g	2	H	H	H	0.046 ± 0.021	0.133 ± 0.009	0.346	2.891
8	8h	2	H	Cl	H	0.044 ± 0.014	0.060 ± 0.004	1.364	0.767
9	8i	2	H	H	Cl	1.829 ± 0.031	1.247 ± 0.041	0.682	1.467
10	8j	2	Me	H	H	0.066 ± 0.005	0.078 ± 0.010	1.182	0.846
11	8k	2	Me	Cl	H	0.068 ± 0.009	0.320 ± 0.005	4.706	0.212
12	8l	2	Me	H	Cl	0.614 ± 0.029	0.487 ± 0.010	1.261	0.793
13	8m	3	H	H	H	0.095 ± 0.014	0.006 ± 0.002	0.063	15.833
14	8n	3	H	Cl	H	0.052 ± 0.026	0.070 ± 0.016	1.346	0.743
15	8o	3	H	H	Cl	0.738 ± 0.022	1.455 ± 0.078	1.971	0.507
16	8p	3	Me	H	H	0.050 ± 0.033	0.038 ± 0.004	0.760	1.316
17	8q	3	Me	Cl	H	0.039 ± 0.021	0.123 ± 0.017	3.154	0.317
18	8r	3	Me	H	Cl	0.273 ± 0.012	3.923 ± 0.029	14.370	0.069
19	Tacrine	–	–	–	–	0.048 ± 0.011	0.010 ± 0.004	0.208	4.800
20	Donepezil	–	–	–	–	0.039 ± 0.097	8.416 ± 0.628	215.795	0.005

^a Inhibitor concentration (mean ± SD of three experiments) required for 50% inactivation of AChE and BChE.

^b Selectivity for AChE is defined as IC₅₀(BChE)/IC₅₀(AChE).

^c Selectivity for BChE is defined as IC₅₀(AChE)/IC₅₀(BChE).

well as the length of methylene linker as they can lead to different lipophilicity and spatial hindrance. Although there is no a definite relation between these factors, generally compounds possessing Cl at 6-position of tetrahydroacridine moiety showed better inhibitory activity than those counterparts in a category. Also, all compounds containing Cl at 7-position of tetrahydroacridine depicted the weakest activity. Another point comes back to the presence of Me group which has not demonstrated a certain role, however, its efficacy has been confirmed in the third category of compounds as compounds **8p-r** are more potent than **8m-o**.

Our results in the case of BChEI activity (Table 1) also can be also discussed in three categories according to the length of methylene linker. In the first series of compounds (**8a-f**), compounds **8c** and **8f** possessing Cl at 7-position of tetrahydroacridine moiety depicted no activity (IC₅₀ > 10) and compound **8a** lacking Cl and Me groups showed the best BChEI activity (IC₅₀ = 0.032 μM). Introduction of Cl into 6-position (compound **8b**) and insertion of Me at 4-position of coumarin (compound **8d**) decreased activity with IC₅₀s = 0.328 and 0.450 μM. However, introduction of Cl along with Me into the desired positions (compound **8e**) showed better inhibitory activity (IC₅₀ = 0.104 μM) than compounds **8b** and **8d**.

In the second category of compounds **8** (**8g-l**), the best anti-BChE activity was depicted by compound **8h** having Cl at 6-position of tetrahydroacridine moiety, however, its counterpart **8k** having methyl group on the coumarin moiety demonstrated lower activity (IC₅₀ = 0.320 μM). Also, compound **8j** showed high activity with IC₅₀ of 0.078 μM which was more active than its counterpart **8g** (IC₅₀ = 0.133 μM). Instructive point refers to compounds **8i** and **8l** which showed good activity (IC₅₀s = 1.247 and 0.487 μM, respectively) comparing with their analogs in the first series (**8c** and **8f**) which were inactive toward BChE. However, the presence of Cl at 6-position of tetrahydroacridine moiety depicted higher BChEI activity than those

compounds possessing Cl at 7-position.

In the third series of compounds (**8m-r**), compound **8m** was the most potent anti-BChE derivative even the most potent compound in the series **8**. However, insertion of Cl at 6- or 7-position of tetrahydroacridine moiety decreased the inhibitory of activity in compounds **8n** and **8o** with IC₅₀s of 0.070 and 1.455 μM, respectively. It should be noted that compounds **8p-r** showed lower activity than their counterparts of **8m-o**, IC₅₀s = 0.038, 0.123, and 3.923 μM, respectively. Hence, derivatives lacking methyl group induced better inhibitory activity than those having that group.

It can be concluded that anti-BChE activity in the first and second groups followed no regularity. Absence and presence of Cl and Me groups as well as the length of methylene linker play complex role in the inhibition of BChE and the effect of linker length cannot be considered as a single factor. It is only clear that chlorine-containing compounds at 7-position of tacrine moiety induced less inhibitory activity than compounds possessing Cl at 6-position or lacking substituent. However, substituents on the tacrine moiety in the third series of compounds affected inhibitory activity in the following order: H > 6-Cl > 7-Cl. Also, the presence of methyl group at 4-position of coumarin usually diminished anti-BChE activity compared with unsubstituted coumarin.

Finally, the affinity of compounds **8b**, **8e**, **8k**, **8q**, and **8r** for AChE was considered by the selectivity index of 5.857, 3.852, 4.706, 3.154, and 14.370, respectively. It was clear that compounds containing chlorine at 6-position of 1,2,3,4-tetrahydroacridine moiety except compound **8r** and methyl group at 4-position of coumarin structure except compound **8b** had high affinity for AChE. Also, compounds **8a**, **8g**, and **8m** showed affinity to BChE by the selectivity index of 5.500, 2.891, and 15.833, respectively. It should be noted that these compounds contained unsubstituted 1,2,3,4-tetrahydroacridine with three, four, and five methylene linkers, respectively. In all series, compounds

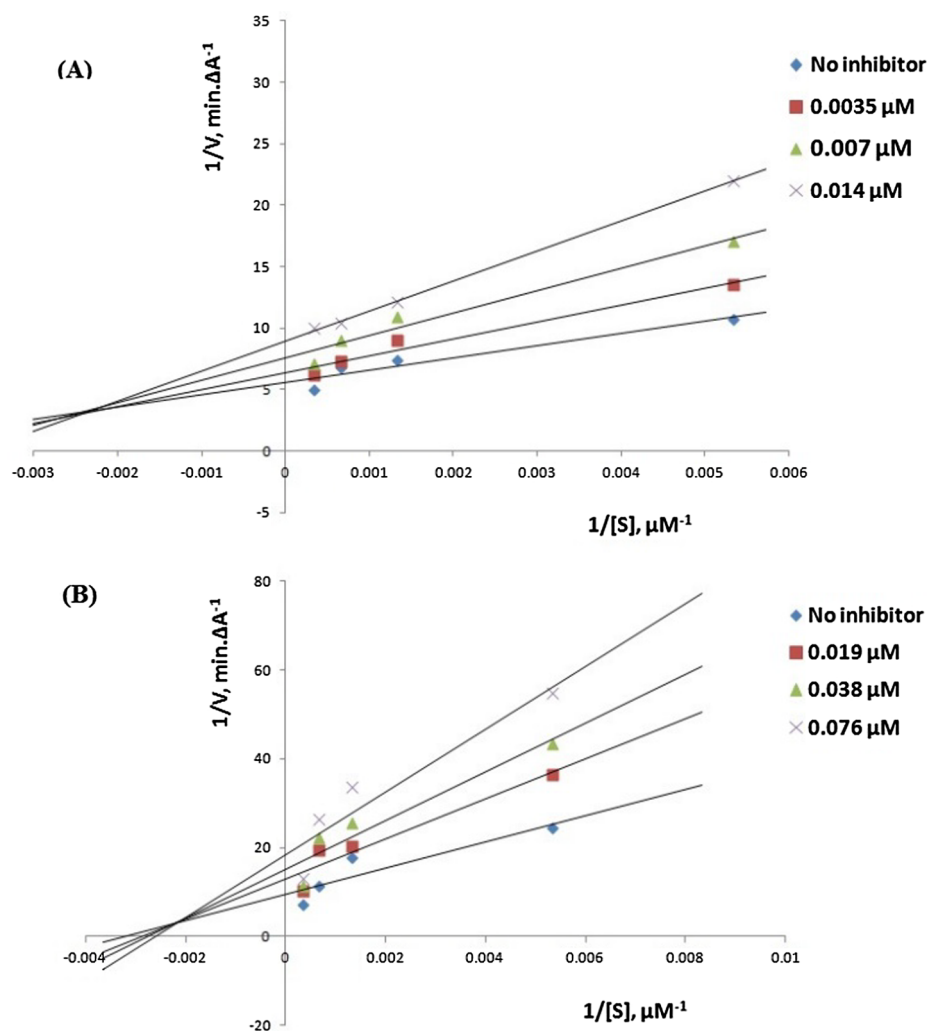


Fig. 2. Kinetic studies of the AChE and BChE inhibition by compound **8e** (A) and **8m** (B), respectively.

bearing 7-Cl substituted 1,2,3,4-tetrahydroacridine ring displayed low inhibitory activity against BChE.

2.2.2. Kinetic studies of AChE and BChE inhibition

The most active compounds toward AChE (**8e**) and BChE (**8m**) were selected for kinetic studies of enzymes inhibition using Lineweaver-Burk plots in the presence of inhibitors (three concentrations) and their absence [24,34]. As can be seen in Fig. 2, graphical analysis of the reciprocal Lineweaver-Burk plots showed both increasing slopes (decreased V_{max}) and intercepts (increased K_{max}) at increasing concentration of both compounds **8e** and **8m** (Fig. 2A and 2B, respectively). The reciprocal plots confirmed mixed type of inhibition for both AChE and BChE suggesting that compounds **8e** and **8m** were able to bind both the CAS and PAS of the AChE and BChE. As seen in Fig. 3A and B, the inhibition constants K_i were calculated for compounds **8e** and **8m** from the secondary plots of the slope versus the concentration of inhibitors (0.061 μM and 0.010 μM , respectively).

2.2.3. BACE1 enzyme inhibitory activity of compound **8e**

BACE1 (β -site APP-cleaving enzyme 1) is considered to be involved in the construction of $A\beta$ peptides. Thus, compound **8e** was selected to be evaluated against BACE1 inhibition [35]. All experiments were repeated for three times and compared with OM99-2. Table 2 indicated that compound **8e** showed moderate inhibitory activity against BACE1 with the percent inhibition of 28.69 and 13.97 at 50 and 10 μM , respectively.

2.2.4. Protection of neuronal PC12 cells against $A\beta$ -induced damage

Neuroprotection effect of compound **8e** against PC12 cells exposed to $A\beta_{25-35}$ was investigated by MTT assay to obtain insight about its neuroprotective properties [35]. Compound **8e** with range concentration of 0.5 to 12.5 μM did not fully protect PC12 cells from neurotoxic effect of $A\beta_{25-35}$ at concentration of 5 μM .

2.3. Docking studies

To investigate the possible interaction modes between active sites of ChEs and the most active compounds, the molecular docking simulations were performed by AutoDock 4.2 and Autodock Vina (AV) 1.1.1 programs [36] with Discovery Studio 4.0 client as shown in Figs. 4–8. The X-ray crystal structures of bifunctional inhibitor bis(7)-tacrine complexed with *Torpedo californica* AChE (PDB Code: 2CKM) and human butyrylcholinesterase in complex with tacrine (PDB Code: 4BDS) were selected to study the molecular modeling [37,38].

The molecular docking studies were carried out for compounds **8e** ($IC_{50} = 0.027 \mu\text{M}$), **8h** ($IC_{50} = 0.044 \mu\text{M}$), and **8q** ($IC_{50} = 0.039 \mu\text{M}$) as potent AChEIs and compounds **8a** ($IC_{50} = 0.032 \mu\text{M}$), **8h** ($IC_{50} = 0.060 \mu\text{M}$), and **8m** ($IC_{50} = 0.006 \mu\text{M}$) as potent BChEIs (Figs. 4–7).

In the case of AChEI activity, our results showed that the orientation of all three compounds were completely similar to native ligand of crystallography (bis(7)-tacrine) with docking score of -13.83 , -13.32 , and -13.71 kcal/mol for compounds **8e**, **8h**, and **8r**, respectively

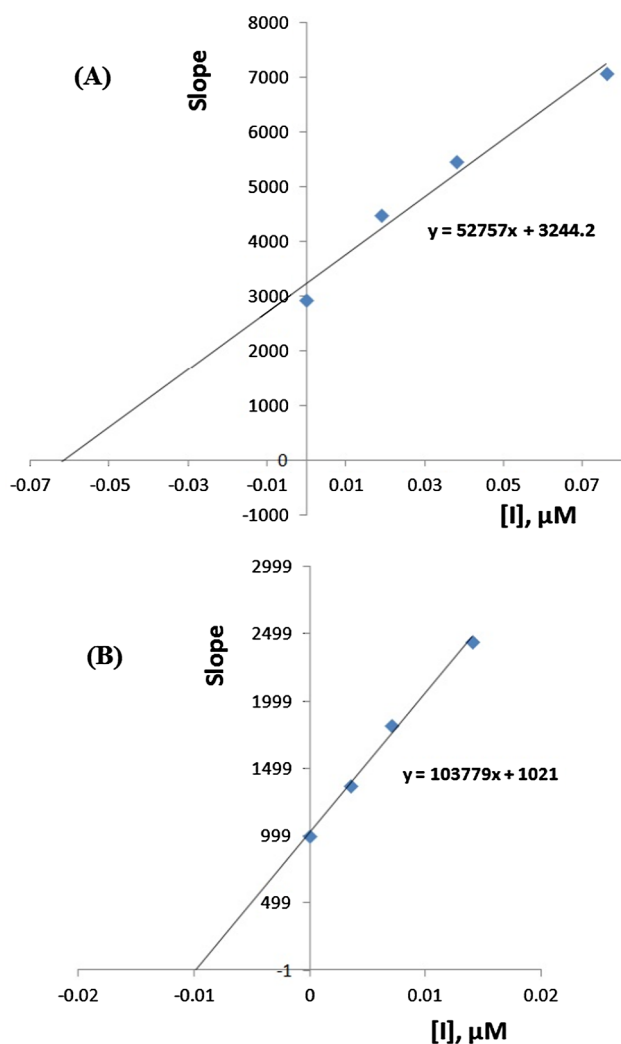


Fig. 3. The Lineweaver-Burk secondary plots of compounds **8e** (A) and **8m** (B).

Table 2
BACE1 inhibitory activity of compound **8e**.

Entry	Compound	Inhibition at 50 μM ^a (%)	Inhibition at 10 μM ^a (%)	IC ₅₀ (nM)
1	8e	28.69 ± 4.79	13.97 ± 12.99	–
2	OM99-2	–	–	14.7 ± 2.83

^a Values represent means ± standard error (S.E.) of three independent experiments.

comparing with docking score of -13.79 kcal/mol for native ligand of crystallography bis(7)-tacrine. Docking scoring showed a good correlation with experimental results as docking score of the most active compound **8e** ($IC_{50} = 0.027$ μM) is slightly more negative than weaker inhibitors **8h** ($IC_{50} = 0.044$ μM) and **8r** ($IC_{50} = 0.039$ μM). All three compounds **8e**, **8h**, and **8q** were long enough to be accommodated in the PAS and CS of the AChE. As can be seen in Fig. 5, the 1,2,3,4-tetrahydroacridine moiety in compound **8e** was placed in the CAS and made a remarkable sandwich π - π stacking with Trp84 and Phe330. Also, chlorine at 6-position of 1,2,3,4-tetrahydroacridine moiety showed a hydrophobic interaction with Trp432, Tyr442, Ile439, Met436 and Phe330. The coumarin moiety was located in the PAS and indicated a sandwich π - π interaction with Trp279 and Tyr70. 1,2,3-Triazole ring was also located in the mid-gorge of AChE between the CAS and PAS and created an anion- π interaction with Asp72.

In the case of BChE activity, compounds **8a** ($IC_{50} = 0.032$ μM), **8h** ($IC_{50} = 0.060$ μM), and **8m** ($IC_{50} = 0.006$ μM) were selected for the molecular docking studies and docking scores were obtained -10.4 , -10.5 , and -10.5 kcal/mol, respectively comparing with docking score of -8.0 kcal/mol for native ligand of crystallography tacrine ($IC_{50} = 0.010$ μM). All compounds were inserted into the active site of BChE and displayed similar interaction mode in the active site of BChE. They demonstrated the same orientation of tacrine as the native ligand (Fig. 6).

Fig. 7 displayed binding mode of the most potent anti-BChE compound **8m** in the active site cleft. The 1,2,3,4-tetrahydroacridine core was located in hydrophobic cavity interacting with amino acid residues Trp82 and Ala328. It made a remarkable π - π interaction with the Trp82 of the CAS. The coumarin core was fitted into ABS of the CS. It displayed π - π and hydrophobic interactions with Trp231 and Leu286. The 1,2,3-triazole ring was oriented directly to the PAS and created the anion- π interaction with Asp70. Also, nitrogen of 1,2,3-triazole ring formed hydrogen bonds with NH of backbone.

2.4. Morris water maze test (MWM)

To evaluate the effect of compound **8e** (the most potent *in vitro* anti-AChE) on memory restoration in scopolamine-induced amnesia [39], the Morris water maze (MWM) test was performed as described in our previous report [24,40]. Scopolamine is a muscarinic cholinergic receptor antagonist which is used to induce memory impairments in animal models. Eleven groups were studied by MWM consisting of a group that received normal saline 5 mL/kg, a vehicle group that received 20% polyethylene glycol 400 (PEG 400), a group that received scopolamine 4 mg/kg, groups that received compound **8e** with doses of 0.3, 0.6, 1.25, 2.5, 5, 10 mg/kg, and two groups that received donepezil 1.25 and 2.5 mg/kg (positive control group). Each rat was subjected to the trial four times (each 90 s) per day for 4 consecutive days in the water maze task to find hidden platform (training days). As shown in Fig. 8(A–C), we evaluated results in terms of escape latency time in Fig. 8A (the time required to find the platform), traveled distance in Fig. 8B (the distance required to find the platform), and swimming speed in Fig. 8C. On the fifth day of the trial (post training probe trial test), platform was removed from the pool and memory was assessed in term of time spent in the target quadrant (Q_1) (Fig. 9).

2.4.1. Effects of compound **8e** administration on escape latency, traveled distance and swimming speed average for all training days

The escape latency (8A), traveled distance (8B) and swimming speed (8C) for all groups in the first 4 days of trials has been shown in Fig. 8. The scopolamine injection produced the significant increase of escape latency ($P < 0.01$) (Fig. 8A) and traveled distance ($P < 0.001$) (Fig. 8B) compared with the saline control. As seen in Fig. 8A and 8B, those groups that received compound **8e** plus scopolamine showed significant improvement in escape latency and traveled distance in comparison to scopolamine administered group. The groups treated with compound **8e** displayed decrease of escape latency including compound **8e** (10 mg/kg) plus scopolamine: $P < 0.01$; compound **8e** (5 mg/kg) plus scopolamine: $P < 0.001$; compound **8e** (2.5 mg/kg) plus scopolamine: $P < 0.01$; compound **8e** (1.25 mg/kg) plus scopolamine: $P < 0.01$; compound **8e** (0.6 mg/kg) plus scopolamine: $P < 0.05$; compound **8e** (0.3 mg/kg) plus scopolamine: $P < 0.05$ in comparison to the scopolamine group (Fig. 8A). The same results were obtained for the traveled distance. The administration of compound **8e** led to significantly decrease in the traveled distance in three groups compared to the scopolamine group (Fig. 8B) (compound **8e** (10 mg/kg) plus scopolamine: $P < 0.001$; compound **8e** (5 mg/kg) plus scopolamine: $P < 0.01$; compound **8e** (2.5 mg/kg) plus scopolamine: $P < 0.001$ and compound **8e** (1.25 mg/kg) plus scopolamine: $P < 0.05$). However, the compound **8e** did not significantly restore the traveled distance with doses of 0.6 and 0.3 mg/kg. It should be noted

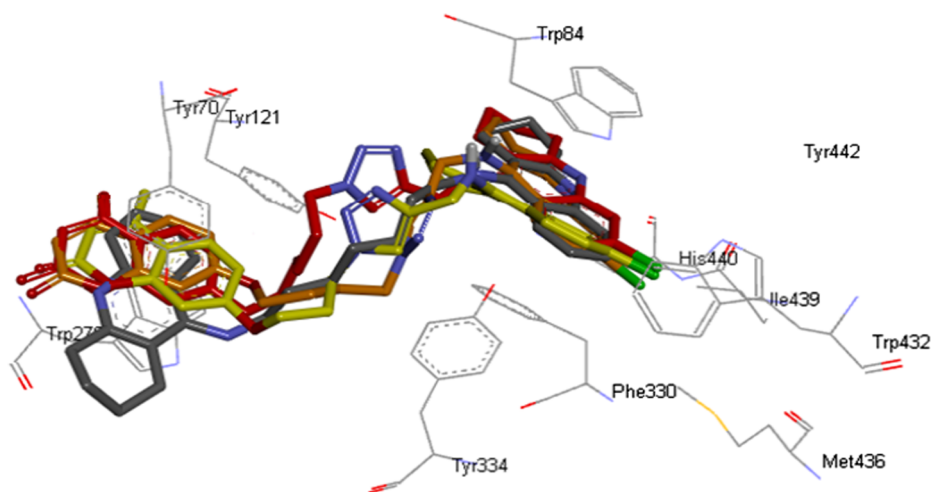


Fig. 4. Superimposition of compounds **8e** (yellow), **8h** (orange), **8q** (red), and bis(7)-tacrine (dark gray) in the active site of AChE.

that swimming speed did not show significant changes in all the groups as shown in Fig. 8C.

2.4.2. Effects of **8e** administration on post training probe trial test

The post-training probe trial test was performed after training days on the fifth day. We left the trained animals in the water for 90 s while the platform was removed and memory was evaluated in term of time spent in the target quadrant (Q1). As seen in Fig. 9, this parameter was significantly decreased for the group that received scopolamine in comparison to the control group ($P < 0.001$) and significantly increased for the groups that received compound **8e** (compound **8e** (10 mg/kg) plus scopolamine: $P < 0.01$; compound **8e** (5 mg/kg) plus scopolamine: $P < 0.001$, compound **8e** (2.5 mg/kg) plus scopolamine: $P < 0.01$), compound **8e** (1.25 mg/kg) plus scopolamine: $P < 0.001$), compound **8e** (0.6 mg/kg) plus scopolamine: $P < 0.01$) and compound **8e** (0.3 mg/kg) plus scopolamine: $P < 0.05$) in comparison to scopolamine group. Also, donepezil plus scopolamine groups with doses of 2.5 and 1.25 mg/kg were applied as positive control and compounds **8e** created significant memory improvement similar to donepezil groups.

3. Conclusion

In conclusion, we reported design and synthesis of a novel series of tacrine-coumarin hybrids linked to 1,2,3-triazoleas potent anti-ChEs. All synthesized compounds showed remarkable inhibitory activity

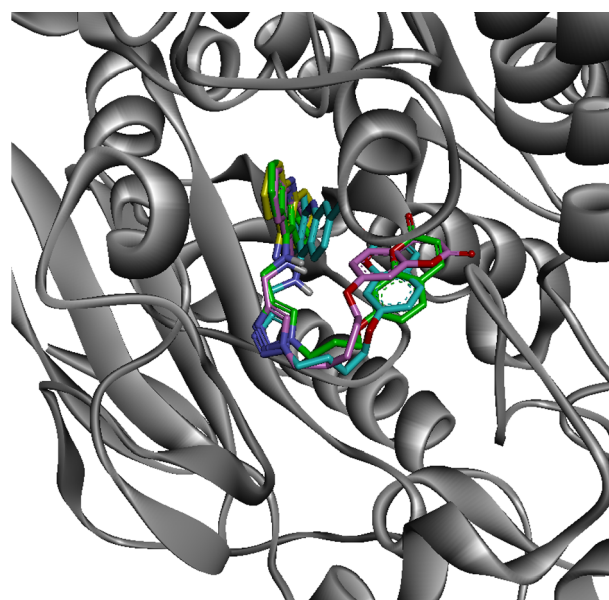


Fig. 6. Proposed binding mode of compounds **8a** (green), **8h** (cyan), **8m** (violet) and tacrine (yellow) in the active site of BChE.

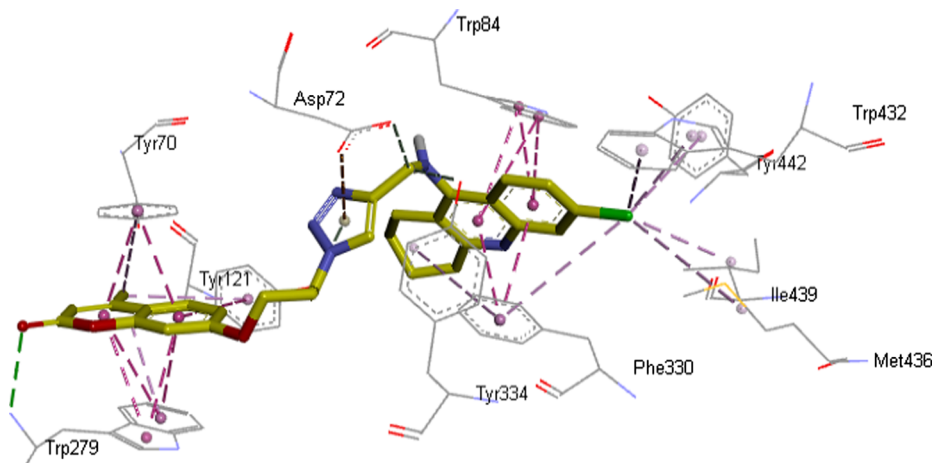


Fig. 5. The binding mode of the most active compound **8e** in the active site of AChE. Hydrogen bonds between carbonyl of coumarin and backbone of Trp279 is shown as green dotted line. Anion- π interaction between Asp72 and 1,2,3-triazole ring is presented as black dotted line. Hydrophobic and π - π interactions are shown as violet dotted lines.

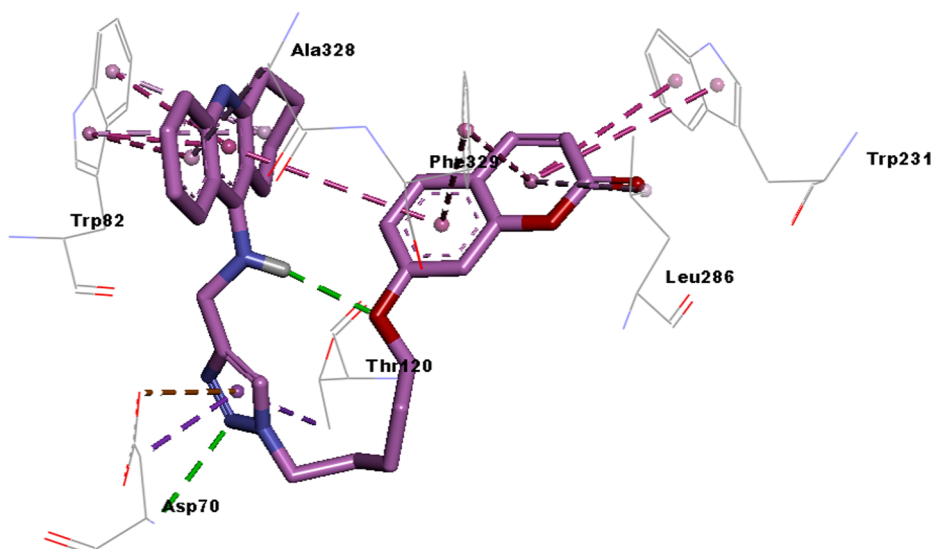


Fig. 7. The binding interaction of the most potent anti-BChE compound **8m** in the cleft of BChE. Hydrogen bonding is shown as green dotted line. Hydrophobic and π - π interactions are shown as violet dotted lines.

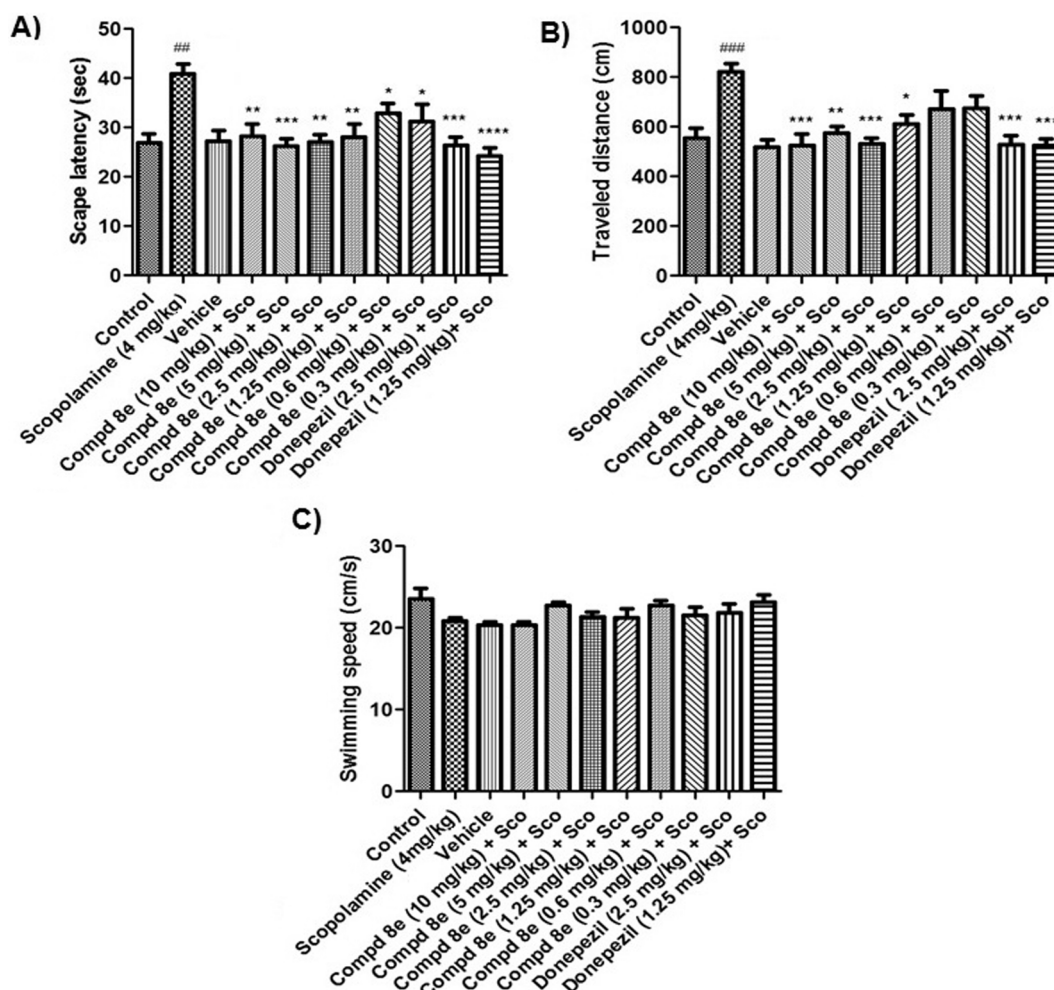


Fig. 8. Effect of compound **8e** plus scopolamine, scopolamine, donepezil, vehicle and saline (control) groups on (A) escape latency, (B) traveled distance and (C) swimming speed in MWM test. Each column displays the mean \pm SEM for seven rats. Sco, scopolamine; * Significantly different from scopolamine groups. # Significantly different from control group. * $P < 0.05$; ** $P < 0.01$; ***, ### $P < 0.001$.

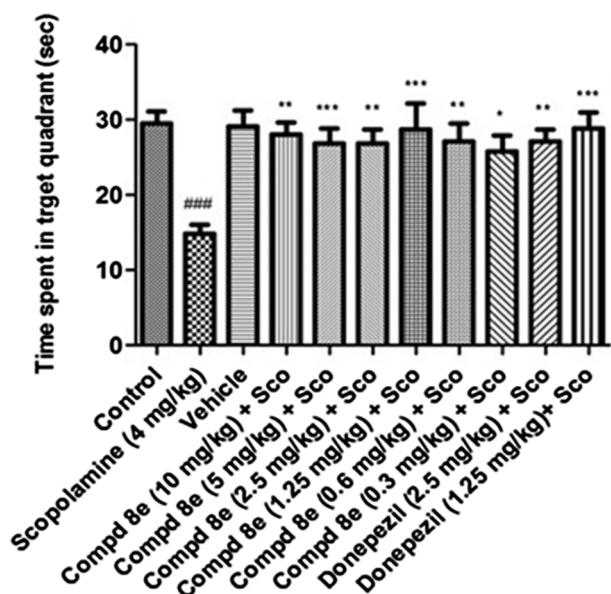


Fig. 9. Effect of compound **8e** on time spent in target quadrant during post training probe trial test in the different groups. Values are expressed as mean \pm SEM for seven animals. Sco, scopolamine; * Significantly different from scopolamine injected group. # Significantly different from control group. * $P < 0.05$, ** $P < 0.01$; ***, ### $P < 0.001$.

toward both AChE and BChE. Among them, compounds **8e** ($IC_{50} = 0.027 \mu M$) and **8m** ($IC_{50} = 0.006 \mu M$) displayed the best anti-AChE and anti-BChE activity, respectively. *In vivo* evaluation of compound **8e** using the Morris Water Maze test showed valuable results based on induction of memory improvement in scopolamine-induced impairment. Also, molecular modeling and kinetics studies showed that compounds **8e** and **8m** bound to both the CS and PAS of AChE and BChE, respectively. Consequently, our results indicated that these novel tacrine-coumarin hybrids may have potential therapeutic benefits for the future of AD treatment.

4. Experimental

Melting points were determined on a Kofler hot stage apparatus and are uncorrected. 1H and ^{13}C NMR spectra were recorded on a Bruker FT-500, using TMS as an internal standard. IR spectra were obtained on a Nicolet Magna FTIR 550 spectrophotometer (KBr disks). MS were recorded on an Agilent Technology (HP) mass spectrometer operating at an ionization potential of 70 eV. Elemental analysis was performed on an Elementar Analysensystem GmbH VarioEL CHNS mode. All chemical were obtained from Merck and Sigma. 4-Methyl-7-hydroxycoumarin (**5b**) was prepared by Pechmann reaction via the condensation of resorcinol and ethylacetoacetate in the presence of concentrated sulfuric acid [28].

4.1. Chemistry

4.1.1. General procedure for the synthesis of compounds **3**, **4**, **6**, **7**

All compounds **3**, **4**, **6**, and **7** are known and were synthesized according to the literature [25–33].

4.1.2. General procedure for the synthesis of compounds **8**

A solution of compounds **7a–f** (0.06 g, 0.9 mmol), compound **4a–c** (1 mmol) and CuI (7 mol%) and trimethylamine (0.13 g, 1.3 mmol) in water (4 mL) and *tert*-butyl alcohol (4 mL) was stirred at room temperature for 12–24 h. Upon completion of the reaction, monitored by TLC, the mixture was diluted with H_2O , extracted with CH_2Cl_2 , and dried over anhydrous Na_2SO_4 . After concentration, the resulting residue

was purified by flash chromatography on silica gel using petroleum ether/ethyl acetate/methanol (1:8:1) as eluent in 48–68% yield.

4.1.2.1. 7-(3-(4-(((1,2,3,4-Tetrahydroacridin-9-yl)amino)methyl)-1H-1,2,3-triazol-1-yl)propoxy)-2H-chromen-2-one (8a). White solid; yield: 68%, mp: 98–100 °C. IR (KBr): 3438, 3134, 2929, 2859, 1729, 1612, 1561, 1502, 1408 cm^{-1} . 1H NMR (500 MHz, $CDCl_3$): 8.02 (d, $J = 8.0$ Hz, 1H, H_8), 7.94 (d, $J = 8.0$ Hz, 1H, H_5), 7.61 (d, $J = 9.5$ Hz, 1H, H_4), 7.61 (d, $J = 8.0$, 1.0 Hz, 1H, H_6), 7.42 (s, 1H, triazole), 7.36–7.33 (m, 2H, H_5 , H_7), 6.76 (dd, $J = 8.5$, 2.5 Hz, 1H, H_6), 6.74 (d, $J = 2.5$ Hz, 1H, H_8), 6.24 (d, $J = 9.5$ Hz, 1H, H_3), 4.8 (s, 2H, $NHCH_2$), 4.55 (t, $J = 6.0$ Hz, 2H, CH_2), 3.98 (t, $J = 6.0$ Hz, 2H, CH_2), 3.05 (t, $J = 5.5$ Hz, 2H, CH_2), 2.70 (t, $J = 5.5$ Hz, 2H, CH_2), 2.39 (quin, $J = 6.0$ Hz, 2H, CH_2), 1.86 (m, 4H, $2 \times CH_2$). ^{13}C NMR (125 MHz, $CDCl_3$): 161.4, 160.9, 159.1, 157.4, 150.8, 147.1, 145.5, 143.2, 129.1, 128.9, 127.1, 124.4, 122.8, 121.8, 119.8, 116.9, 113.4, 112.9, 112.5, 101.6, 64.7, 47.7, 44.3, 32.8, 29.6, 24.5, 22.7, 22.3. Anal. Calcd for $C_{28}H_{27}N_5O_3$: C, 69.84; H, 5.65; N, 14.54. Found: C, 70.06; H, 5.88; N, 14.39.

4.1.2.2. 7-(3-(4-(((6-Chloro-1,2,3,4-tetrahydroacridin-9-yl)amino)methyl)-1H-1,2,3-triazol-1-yl)propoxy)-2H-chromen-2-one(8b). White solid, yield: 51%, mp: 100–102 °C. IR (KBr): 3388, 3171, 2943, 2861, 1724, 1609, 1556, 1507, 1481 cm^{-1} . 1H NMR (500 MHz, $DMSO-d_6$): 8.16 (d, $J = 9.0$ Hz, 1H, H_8), 7.96 (d, $J = 9.5$ Hz, 1H, H_4), 7.94 (s, 1H, triazole), 7.71 (s, 1H, H_5), 7.59 (d, $J = 8.5$ Hz, 1H, H_5), 7.29 (d, $J = 9.0$ Hz, 1H, H_7), 6.9 (s, 1H, H_8), 6.87 (d, $J = 8.5$ Hz, 1H, H_6), 6.27 (d, $J = 9.5$ Hz, 1H, H_3), 5.93 (t, $J = 7.0$ Hz, 1H, NH), 4.64 (d, $J = 7.0$ Hz, 2H, $NHCH_2$), 4.49 (t, $J = 6.0$ Hz, 2H, CH_2), 3.98 (t, $J = 6.0$ Hz, 2H, CH_2), 2.87 (t, $J = 5.5$ Hz, 2H, CH_2), 2.71 (t, $J = 5.5$ Hz, 2H, CH_2), 2.22 (quin, $J = 6.0$ Hz, 2H, CH_2), 1.76 (m, 4H, $2 \times CH_2$). ^{13}C NMR (125 MHz, $DMSO-d_6$): 161.3, 160.1, 159.5, 155.2, 149.8, 147.4, 145.7, 144.1, 132.3, 129.4, 129.3, 126.7, 125.3, 123.5, 122.8, 118.9, 117.2, 112.5, 112.4, 101.2, 65.0, 46.1, 42.9, 33.4, 29.1, 24.7, 22.4, 22.1. Anal. Calcd for $C_{28}H_{26}ClN_5O_3$: C, 65.18; H, 5.08; N, 13.57. Found: C, 65.32; H, 5.21; N, 13.39.

4.1.2.3. 7-(3-(4-(((7-Chloro-1,2,3,4-tetrahydroacridin-9-yl)amino)methyl)-1H-1,2,3-triazol-1-yl)propoxy)-2H-chromen-2-one (8c). White solid; yield: 59%, mp: 100–102 °C. IR (KBr): 3414, 3133, 2935, 2870, 1728, 1620, 1555, 1503, 1468 cm^{-1} . 1H NMR (500 MHz, CD_3Cl): 7.93 (d, $J = 2.0$ Hz, 1H, H_8), 7.84 (d, $J = 9.0$ Hz, 1H, H_5), 7.60 (d, $J = 9.5$ Hz, 1H, H_4), 7.47 (d, $J = 9.0$, 2.0 Hz, 1H, H_6), 7.34 (d, $J = 8.5$ Hz, 1H, H_5), 7.31 (s, 1H, triazole), 6.78–6.75 (m, 2H, H_6 , H_8), 6.24 (d, $J = 9.5$ Hz, 1H, H_3), 4.66 (d, $J = 7.0$ Hz, 2H, $NHCH_2$), 4.55 (t, $J = 6.0$ Hz, 2H, CH_2), 3.99 (t, $J = 6.0$ Hz, 2H, CH_2), 3.01 (t, $J = 6.0$ Hz, 2H, CH_2), 2.71 (t, $J = 6.0$ Hz, 2H, CH_2), 2.40 (quin, $J = 6.0$ Hz, 2H, CH_2), 1.86 (m, 4H, $2 \times CH_2$). ^{13}C NMR (125 MHz, $CDCl_3$): 161.4, 160.8, 159.3, 155.8, 149.1, 145.8, 145.6, 143.1, 130.6, 129.8, 129.1, 128.9, 122.9, 121.8, 121.5, 119.1, 113.5, 113.0, 112.4, 101.6, 64.6, 46.9, 44.3, 34.0, 29.6, 24.6, 22.8, 22.6. Anal. Calcd for $C_{28}H_{26}ClN_5O_3$: C, 65.18; H, 5.08; N, 13.57. Found: C, 64.97; H, 4.92; N, 13.41.

4.1.2.4. 4-Methyl-7-(3-(4-(((1,2,3,4-tetrahydroacridin-9-yl)amino)methyl)-1H-1,2,3-triazol-1-yl)propoxy)-2H-chromen-2-one (8d). White solid; yield: 48%, mp: 98–100 °C. IR (KBr): 3411, 3134, 2932, 2855, 1708, 1617, 1578, 1511, 1431 cm^{-1} . 1H NMR (500 MHz, $DMSO-d_6$): 8.12 (d, $J = 8.5$ Hz, 1H, H_8), 7.93 (s, 1H, triazole), 7.70 (d, $J = 8.5$ Hz, 1H, H_5), 7.65 (d, $J = 8.5$ Hz, 1H, H_5), 7.50 (t, $J = 8.5$, 1.0 Hz, 1H, H_6), 7.31 (t, $J = 8.5$ Hz, 1H, H_7), 6.91 (d, $J = 2.5$ Hz, 1H, H_8), 6.89 (dd, $J = 8.5$, 2.5 Hz, 1H, H_6), 6.20 (s, 1H, H_3), 5.77 (t, $J = 7.0$ Hz, 1H, NH), 4.60 (d, $J = 7.0$ Hz, 2H, $NHCH_2$), 4.48 (t, $J = 6.0$ Hz, 2H, CH_2), 3.98 (t, $J = 6.0$ Hz, 2H, CH_2), 2.88 (t, $J = 5.5$ Hz, 2H, CH_2), 2.72 (t, $J = 5.5$ Hz, 2H, CH_2), 2.38 (s, 2H, CH_3), 2.22 (quin, $J = 6.0$ Hz, 2H, CH_2), 1.77 (m, 4H, $2 \times CH_2$). ^{13}C NMR (125 MHz, $CDCl_3$): 161.2, 160.1, 158.0, 155.6, 152.3, 150.1, 147.2, 145.8, 128.6, 128.3, 125.7, 124.3, 122.6, 121.6,

120.3, 118.2, 114.0, 112.3, 112.1, 101.6, 64.6, 46.9, 44.2, 33.6, 29.6, 24.7, 22.8, 22.6, 18.5. Anal. Calcd for $C_{29}H_{29}N_5O_3$: C, 70.28; H, 5.90; N, 14.13. Found: C, 70.41; H, 6.08; N, 14.21.

4.1.2.5. 7-(3-(4-(((6-Chloro-1,2,3,4-tetrahydroacridin-9-yl)amino)methyl)-1H-1,2,3-triazol-1-yl)propoxy)-4-methyl-2H-chromen-2-one (8e). White solid; yield: 68%, mp 125–127 °C. IR (KBr): 3401, 3151, 2929, 2862, 1724, 1613, 1559, 1488 cm^{-1} . 1H NMR (500 MHz, $CDCl_3$): 7.90 (d, $J = 9.0$ Hz, 1H, H_8), 7.89 (s, 1H, H_5), 7.47 (d, $J = 8.5$ Hz, 1H, H_5), 7.27 (d, $J = 9.0$ Hz, 1H, H_7), 7.26 (s, 1H, triazole), 6.78 (dd, $J = 8.5, 2.0$ Hz, 1H, H_6), 6.74 (d, $J = 2.0$ Hz, 1H, H_8), 6.13 (s, 1H, H_3), 4.68 (s, 1H, $NHCH_2$), 4.54 (t, $J = 6.0$ Hz, 2H, CH_2), 3.98 (t, $J = 6.0$ Hz, 2H, CH_2), 3.01 (t, $J = 5.5$ Hz, 2H, CH_2), 2.69 (t, $J = 5.5$ Hz, 2H, CH_2), 2.41–2.36 (m, 5H, CH_3 , CH_2), 1.86 (m, 4H, $2 \times CH_2$). ^{13}C NMR (125 MHz, $CDCl_3$): 161.2, 160.9, 160.1, 157.1, 152.2, 149.9, 147.9, 145.6, 134.1, 127.7, 125.7, 124.9, 124.2, 121.5, 119.0, 118.2, 114.0, 112.3, 112.1, 101.6, 64.6, 46.9, 44.3, 34.0, 29.6, 24.6, 22.8, 22.6, 18.5. Anal. Calcd for $C_{29}H_{28}ClN_5O_3$: C, 65.72; H, 5.32; N, 13.21. Found: C, 65.58; H, 5.17; N, 13.06.

4.1.2.6. 7-(3-(4-(((7-Chloro-1,2,3,4-tetrahydroacridin-9-yl)amino)methyl)-1H-1,2,3-triazol-1-yl)propoxy)-4-methyl-2H-chromen-2-one (8f). Cream solid; yield: 64%, mp 87–89 °C. IR (KBr): 3424, 3133, 2928, 2859, 1713, 1612, 1561, 1487 cm^{-1} . 1H NMR (500 MHz, $CDCl_3$): 7.92 (d, $J = 2.0$ Hz, 1H, H_8), 7.82 (d, $J = 9.0$ Hz, 1H, H_5), 7.47–7.44 (m, 2H, H_5 , H_6), 7.34 (s, 1H, triazole), 6.78 (dd, $J = 9.0, 2.0$ Hz, 1H, H_6), 6.78 (d, $J = 2.0$ Hz, 1H, H_8), 6.10 (s, 1H, H_3), 4.65 (s, 2H, $NHCH_2$), 4.56 (t, $J = 6.0$ Hz, 2H, CH_2), 3.99 (t, $J = 6.0$ Hz, 2H, CH_2), 3.00 (t, $J = 6.5$ Hz, 2H, CH_2), 2.71 (t, $J = 6.5$ Hz, 2H, CH_2), 2.41–2.33 (m, 2H, CH_3 , CH_2), 1.86 (m, 4H, $2 \times CH_2$). ^{13}C NMR (125 MHz, $CDCl_3$): 161.2, 160.9, 159.3, 155.1, 152.2, 149.1, 145.8, 145.6, 130.6, 129.6, 129.0, 125.6, 121.7, 121.6, 121.5, 119.0, 113.9, 112.2, 112.0, 101.6, 64.6, 46.9, 44.3, 34.0, 29.6, 24.5, 22.7, 22.6, 18.51. Anal. Calcd for $C_{29}H_{28}ClN_5O_3$: C, 65.72; H, 5.32; N, 13.21. Found: C, 65.88; H, 5.50; N, 13.37.

4.1.2.7. 7-(4-(4-(((1,2,3,4-Tetrahydroacridin-9-yl)amino)methyl)-1H-1,2,3-triazol-1-yl)butoxy)-2H-chromen-2-one (8g). cream solid; yield: 54%, mp 78–80 °C. IR (KBr): 3384, 3128, 2926, 2855, 1727, 1611, 1564, 1504, 1411 cm^{-1} . 1H NMR (500 MHz, $CDCl_3$): 8.06 (d, $J = 8.0$ Hz, 1H, H_8), 7.97 (d, $J = 8.0$ Hz, 1H, H_5), 7.60 (d, $J = 9.5$ Hz, 1H, H_4), 7.55 (t, $J = 8.0$ Hz, 1H, H_6), 7.41 (s, 1H, triazole), 7.36 (t, $J = 8.0$ Hz, 1H, H_7), 7.35 (d, $J = 8.5$ Hz, 1H, H_5), 6.79 (dd, $J = 8.5, 2.0$ Hz, 1H, H_6), 6.75 (d, $J = 2.0$ Hz, 1H, H_8), 6.23 (d, $J = 9.5$ Hz, 1H, H_3), 4.82 (s, 2H, $NHCH_2$), 4.40 (t, $J = 6.0$ Hz, 2H, CH_2), 4.00 (t, $J = 7.0$ Hz, 2H, CH_2), 3.06 (t, $J = 7.0$ Hz, 2H, CH_2), 2.72 (t, $J = 6.0$ Hz, 2H, CH_2), 2.08 (quin, $J = 6.0$ Hz, 2H, CH_2), 1.86 (m, 4H, $2 \times CH_2$), 1.77 (quin, $J = 7.0$ Hz, 2H, CH_2). ^{13}C NMR (125 MHz, $CDCl_3$): 161.8, 160.9, 159.3, 154.5, 150.6, 148.1, 145.3, 143.2, 129.1, 128.8, 127.0, 124.8, 124.4, 123.0, 121.5, 119.7, 116.9, 113.3, 112.7, 101.4, 67.5, 49.9, 44.1, 32.8, 27.0, 25.9, 24.6, 22.7, 22.3. Anal. Calcd for $C_{29}H_{29}N_5O_3$: C, 70.28; H, 5.90; N, 14.13. Found: C, 70.07; H, 5.76; N, 14.02.

4.1.2.8. 7-(4-(4-(((6-chloro-1,2,3,4-tetrahydroacridin-9-yl)amino)methyl)-1H-1,2,3-triazol-1-yl)butoxy)-2H-chromen-2-one (8h). Cream solid; yield: 49%, mp 121–124 °C. IR (KBr): 3314, 3147, 2931, 2869, 1730, 1617, 1553, 1501, 1471 cm^{-1} . 1H NMR (500 MHz, $CDCl_3$): 7.91 (d, $J = 9.0$ Hz, 1H, H_8), 7.86 (d, $J = 2.0$ Hz, 1H, H_5), 7.59 (d, $J = 9.5$ Hz, 1H, H_4), 7.33 (d, $J = 8.5$ Hz, 1H, H_5), 7.29 (s, 1H, triazole), 7.28 (dd, $J = 9.0, 2.0$ Hz, 1H, H_7), 6.77 (d, $J = 8.5, 2.0$ Hz, 1H, H_6), 6.72 (d, $J = 8.5$ Hz, 1H, H_8), 6.21 (d, $J = 9.5$ Hz, 1H, H_3), 4.67 (s, 2H, $NHCH_2$), 4.39 (t, $J = 7.0$ Hz, 2H, CH_2), 3.98 (t, $J = 7.0$ Hz, 2H, CH_2), 2.99 (t, $J = 6.0$ Hz, 2H, CH_2), 2.69 (t, $J = 6.0$ Hz, 2H, CH_2), 2.06 (quin, $J = 7.0$ Hz, 2H, CH_2), 1.86 (m, 4H, $2 \times CH_2$), 1.74 (quin, $J = 7.0$ Hz, 2H, CH_2). ^{13}C NMR (125 MHz, $CDCl_3$): 161.7, 160.9,

160.0, 155.7, 149.8, 147.9, 145.5, 143.1, 133.9, 128.7, 127.7, 124.7, 124.1, 121.1, 119.0, 118.2, 113.3, 113.0, 112.5, 101.3, 67.4, 49.8, 44.2, 34.0, 26.9, 25.8, 24.5, 22.7, 22.5. Anal. Calcd for $C_{29}H_{28}ClN_5O_3$: C, 65.72; H, 5.32; N, 13.21. Found: C, 65.42; H, 5.21; N, 13.39.

4.1.2.9. 7-(4-(4-(((7-Chloro-1,2,3,4-tetrahydroacridin-9-yl)amino)methyl)-1H-1,2,3-triazol-1-yl)butoxy)-2H-chromen-2-one (8i). Cream solid; yield: 62%, mp 70–72 °C. IR (KBr): 3382, 3141, 2933, 2860, 1728, 1612, 1556, 1487 cm^{-1} . 1H NMR (500 MHz, $DMSO-d_6$): 8.21 (s, 1H, triazole), 7.96 (d, $J = 9.0$ Hz, 1H, H_5), 7.90 (s, 1H, H_8), 7.71 (d, $J = 9.5$ Hz, 1H, H_4), 7.60 (d, $J = 8.5$ Hz, 1H, H_5), 7.49 (d, $J = 9.0$ Hz, 1H, H_6), 6.93 (s, 1H, H_8), 6.24 (d, $J = 8.5, 2.0$ Hz, 1H, H_6), 6.27 (d, $J = 9.5$ Hz, 1H, H_3), 6.0 (t, $J = 7.0$ Hz, 1H, $NHCH_2$), 4.60 (d, $J = 7.0$ Hz, 2H, $NHCH_2$), 4.37 (t, $J = 6.0$ Hz, 2H, CH_2), 4.02 (t, $J = 6.0$ Hz, 2H, CH_2), 2.89 (t, $J = 6.0$ Hz, 2H, CH_2), 2.76 (t, $J = 6.0$ Hz, 2H, CH_2), 1.89 (quin, $J = 6.0$ Hz, 2H, CH_2), 1.76 (m, 4H, $2 \times CH_2$), 1.57 (quin, $J = 6.0$ Hz, 2H, CH_2). ^{13}C NMR (125 MHz, $DMSO-d_6$): 161.6, 160.1, 158.8, 155.3, 148.9, 145.7, 145.1, 144.1, 130.3, 129.3, 129.2, 128.2, 128.0, 122.6, 121.8, 121.4, 118.2, 112.6, 112.4, 101.1, 67.4, 48.7, 42.6, 33.4, 26.3, 25.2, 25.1, 22.4, 22.1. Anal. Calcd for $C_{29}H_{28}ClN_5O_3$: C, 65.72; H, 5.32; N, 13.21. Found: C, 65.88; H, 5.50; N, 13.34.

4.1.2.10. 4-Methyl-7-(4-(4-(((1,2,3,4-tetrahydroacridin-9-yl)amino)methyl)-1H-1,2,3-triazol-1-yl)butoxy)-2H-chromen-2-one (8j). Cream solid; yield: 61%, mp 60–62 °C. IR (KBr): 3390, 3139, 2926, 2855, 1716, 1613, 1577, 1419 cm^{-1} . 1H NMR (500 MHz, $CDCl_3$): 7.91 (d, $J = 8.5$ Hz, 1H, H_8), 7.84 (d, $J = 8.5$ Hz, 1H, H_5), 7.47 (t, $J = 8.5$ Hz, 1H, H_6), 7.39 (d, $J = 8.5$ Hz, 1H, H_5), 7.29 (t, $J = 8.5$ Hz, 1H, H_7), 7.19 (s, 1H, triazole), 6.73 (dd, $J = 9.0, 2.5$ Hz, 1H, H_6), 6.67 (d, $J = 2.5$ Hz, 1H, H_8), 6.03 (s, 1H, H_3), 4.63 (s, 2H, $NHCH_2$), 4.30 (t, $J = 6.0$ Hz, 2H, CH_2), 3.91 (t, $J = 6.0$ Hz, 2H, CH_2), 2.96 (t, $J = 6.0$ Hz, 2H, CH_2), 2.64 (t, $J = 6.0$ Hz, 2H, CH_2), 2.29 (s, 2H, CH_3), 1.98 (quin, $J = 6.0$ Hz, 2H, CH_2), 1.78 (m, 4H, $2 \times CH_2$), 1.98 (quin, $J = 6.0$ Hz, 2H, CH_2). ^{13}C NMR (125 MHz, $CDCl_3$): 161.6, 161.0, 158.7, 155.2, 152.3, 149.8, 147.2, 145.8, 128.7, 128.4, 125.5, 124.2, 122.5, 121.1, 120.7, 118.1, 113.7, 112.3, 112.0, 101.4, 64.4, 49.8, 44.2, 33.9, 27.0, 25.8, 24.7, 22.9, 22.7, 18.2. Anal. Calcd for $C_{30}H_{30}N_5O_3$: C, 70.71; H, 6.13; N, 13.74. Found: C, 70.58; H, 6.01; N, 13.60.

4.1.2.11. 7-(4-(4-(((6-Chloro-1,2,3,4-tetrahydroacridin-9-yl)amino)methyl)-1H-1,2,3-triazol-1-yl)butoxy)-4-methyl-2H-chromen-2-one (8k). White solid; yield: 68%, mp 134–136 °C. IR (KBr): 3355, 3129, 2932, 1712, 1611, 1574, 1419 cm^{-1} . 1H NMR (500 MHz, $DMSO-d_6$): 8.17 (d, $J = 9.0$ Hz, 1H, H_8), 7.88 (s, H, triazole), 7.70 (d, $J = 2.0$ Hz, 1H, H_5), 7.66 (d, $J = 8.5$ Hz, 1H, H_5), 7.32 (d, $J = 8.5$ Hz, 1H, H_7), 6.93–6.91 (m, 2H, H_6 , H_8), 6.19 (s, 1H, H_3), 5.99 (t, $J = 7.0$ Hz, 1H, $NHCH_2$), 4.63 (d, $J = 7.0$ Hz, 2H, $NHCH_2$), 4.36 (t, $J = 6.0$ Hz, 2H, CH_2), 4.02 (t, $J = 6.0$ Hz, 2H, CH_2), 2.87 (t, $J = 6.0$ Hz, 2H, CH_2), 2.71 (t, $J = 6.0$ Hz, 2H, CH_2), 2.38 (s, 3H, CH_3), 1.89 (quin, $J = 6.0$ Hz, 2H, CH_2), 1.716 (m, 4H, $2 \times CH_2$), 1.58 (quin, $J = 6.0$ Hz, 2H, CH_2). ^{13}C NMR (125 MHz, $DMSO-d_6$): 161.5, 160.2, 159.5, 154.6, 153.2, 149.8, 147.4, 145.6, 132.3, 126.7, 126.3, 125.4, 123.6, 122.6, 119.0, 117.3, 113.1, 112.2, 111.1, 101.2, 64.4, 48.7, 42.8, 33.4, 26.3, 25.2, 24.8, 22.4, 22.1, 18.0. Anal. Calcd for $C_{30}H_{30}ClN_5O_3$: C, 66.23; H, 5.56; N, 12.58. Found: C, 66.39; H, 5.71; N, 12.72.

4.1.2.12. 7-(4-(4-(((7-Chloro-1,2,3,4-tetrahydroacridin-9-yl)amino)methyl)-1H-1,2,3-triazol-1-yl)butoxy)-4-methyl-2H-chromen-2-one (8l). White solid; yield: 67%, mp 122–124 °C. IR (KBr): 3388, 3144, 2930, 2862, 1713, 1610, 1575, 1486, 1424 cm^{-1} . 1H NMR (500 MHz, $CDCl_3$): 7.97 (s, 1H, H_8), 7.86 (d, $J = 8.5$ Hz, 1H, H_5), 7.48–7.45 (m, 2H, H_5 , H_6), 7.37 (s, 1H, triazole), 6.78 (d, $J = 9.0$ Hz, 1H, H_6), 6.74 (s, 1H, H_8), 6.10 (s, 1H, H_3), 4.70 (s, 2H, $NHCH_2$), 4.42 (t, $J = 6.0$ Hz, 2H, CH_2), 4.00 (t, $J = 6.0$ Hz, 2H, CH_2), 3.02 (t, $J = 6.0$ Hz, 2H, CH_2), 2.71 (t, $J = 6.0$ Hz, 2H, CH_2), 2.36 (s, 3H, CH_3), 2.09 (quin, $J = 6.0$ Hz, 2H,

CH₂), 1.86 (m, 4H, 2 × CH₂), 1.77 (quin, *J* = 6.0 Hz, 2H, CH₂). ¹³C NMR (125 MHz, CDCl₃): 161.6, 161.07, 158.8, 155.2, 149.4, 145.4, 145.2, 145.6, 130.0, 129.8, 129.3, 125.5, 121.9, 121.2, 120.5, 118.7, 113.7, 112.3, 112.0, 101.3, 64.4, 49.9, 44.2, 33.6, 27.0, 25.9, 24.5, 22.6, 22.4, 18.3. Anal. Calcd for C₃₀H₃₀ClN₅O₃: C, 65.72; H, 5.32; N, 13.21. Found: C, 65.88; H, 5.50; N, 13.37.

4.1.2.13. 7-((5-(4-(((1,2,3,4-Tetrahydroacridin-9-yl)amino)methyl)-1H-1,2,3-triazol-1-yl)pentyl)oxy)-2H-chromen-2-one (**8m**). Brown gum-solid; yield: 64%. IR (KBr): 3391, 3125, 2923, 2840, 1726, 1616, 1556, 1493 cm⁻¹. ¹H NMR (500 MHz, CDCl₃): 7.99 (d, *J* = 8.5 Hz, 1H, H₈), 7.91 (d, *J* = 8.5 Hz, 1H, H₅), 7.59 (d, *J* = 9.5 Hz, 1H, H₄), 7.54 (t, *J* = 8.5 Hz, 1H, H₆), 7.35 (t, *J* = 8.5 Hz, 1H, H₇), 7.33 (d, *J* = 8.5 Hz, 1H, H₅), 7.28 (s, 1H, triazole), 6.77 (d, *J* = 8.5 Hz, 1H, H₆), 6.74 (s, 1H, H₈), 6.23 (d, *J* = 9.5 Hz, 1H, H₃), 4.71 (s, 2H, NHCH₂), 4.32 (t, *J* = 6.0 Hz, 2H, CH₂), 3.96 (t, *J* = 6.0 Hz, 2H, CH₂), 3.03 (t, *J* = 6.0 Hz, 2H, CH₂), 2.71 (t, *J* = 6.0 Hz, 2H, CH₂), 1.93–1.79 (m, 8H, 4 × CH₂), 1.44 (quin, *J* = 6.0 Hz, 2H, CH₂). ¹³C NMR (125 MHz, CDCl₃): 162.0, 160.9, 158.6, 155.8, 149.9, 147.0, 145.7, 143.2, 128.7, 128.5, 128.3, 124.1, 122.5, 121.0, 120.6, 117.9, 112.9, 112.7, 112.5, 101.3, 67.9, 50.0, 44.2, 33.8, 29.8, 28.2, 24.6, 22.9, 22.8, 22.6. Anal. Calcd for C₃₀H₃₁N₅O₃: C, 70.71; H, 6.13; N, 13.74. Found: C, 70.57; H, 5.98; N, 13.57.

4.1.2.14. 7-((5-(4-(((6-Chloro-1,2,3,4-tetrahydroacridin-9-yl)amino)methyl)-1H-1,2,3-triazol-1-yl)pentyl)oxy)-2H-chromen-2-one (**8n**). Brown gum-solid; yield: 54%. IR (KBr): 3348, 3133, 2928, 2862, 1731, 1615, 1541, 1489 cm⁻¹. ¹H NMR (500 MHz, CDCl₃): 7.92 (d, *J* = 9.0 Hz, 1H, H₈), 7.86 (s, 1H, H₅), 7.59 (d, *J* = 9.5 Hz, 1H, H₄), 7.32–7.25 (m, 3H, H₅, H₇, triazole), 6.77 (d, *J* = 8.5 Hz, 1H, H₆), 6.72 (s, 1H, H₈), 6.19 (d, *J* = 9.5 Hz, 1H, H₃), 4.68 (s, 2H, NHCH₂), 4.34 (t, *J* = 6.0 Hz, 2H, CH₂), 3.96 (t, *J* = 6.0 Hz, 2H, CH₂), 2.99 (s, 2H, CH₂), 2.69 (s, 2H, CH₂), 1.93–1.84 (m, 8H, 4 × CH₂), 1.45 (quin, *J* = 6.0 Hz, 2H, CH₂). ¹³C NMR (125 MHz, CDCl₃): 161.9, 160.9, 159.9, 155.7, 149.8, 147.8, 145.4, 143.2, 133.9, 128.6, 127.6, 124.6, 124.1, 121.0, 118.9, 118.0, 112.9, 112.6, 112.4, 101.2, 67.8, 50.0, 44.2, 33.9, 29.7, 28.1, 24.5, 22.9, 22.7, 22.5. Anal. Calcd for C₃₀H₃₀ClN₅O₃: C, 66.23; H, 5.56; N, 12.87. Found: C, 66.11; H, 5.39; N, 12.69.

4.1.2.15. 7-((5-(4-(((7-Chloro-1,2,3,4-tetrahydroacridin-9-yl)amino)methyl)-1H-1,2,3-triazol-1-yl)pentyl)oxy)-2H-chromen-2-one (**8o**). Brown gum-solid; yield: 60%. IR (KBr): 3359, 3127, 2941, 2852, 1720, 1619, 1503, 1487 cm⁻¹. ¹H NMR (500 MHz, CDCl₃): 7.96 (s, 1H, H₈), 7.82 (d, *J* = 8.5 Hz, 1H, H₅), 7.58 (d, *J* = 9.5 Hz, 1H, H₄), 7.45 (d, *J* = 8.5 Hz, 1H, H₅), 7.36 (s, 1H, triazole), 7.31 (d, *J* = 8.5 Hz, 1H, H₆), 6.77 (d, *J* = 8.5 Hz, 1H, H₆), 6.71 (s, 1H, H₈), 6.19 (d, *J* = 9.5 Hz, 1H, H₃), 4.67 (s, 2H, NHCH₂), 4.35 (t, *J* = 6.0 Hz, 2H, CH₂), 3.96 (t, *J* = 6.0 Hz, 2H, CH₂), 3.00 (s, 2H, CH₂), 2.70 (s, 2H, CH₂), 1.94 (quin, *J* = 6.0 Hz, 2H, CH₂), 1.84 (m, 8H, 4 × CH₂), 1.46 (quin, *J* = 6.0 Hz, 2H, CH₂). ¹³C NMR (125 MHz, CDCl₃): 161.9, 160.9, 159.0, 155.7, 149.1, 145.6, 145.4, 143.2, 130.3, 129.5, 128.9, 128.6, 121.7, 121.3, 121.0, 118.8, 112.8, 112.6, 112.4, 101.2, 67.8, 49.9, 44.2, 33.8, 29.7, 28.1, 24.5, 22.9, 22.6, 22.4. Anal. Calcd for C₃₀H₃₀ClN₅O₃: C, 66.23; H, 5.56; N, 12.87. Found: C, 66.08; H, 5.41; N, 12.71.

4.1.2.16. 4-Methyl-7-((5-(4-(((1,2,3,4-tetrahydroacridin-9-yl)amino)methyl)-1H-1,2,3-triazol-1-yl)pentyl)oxy)-2H-chromen-2-one (**8p**). Brown gum-solid; yield: 63%. IR (KBr): 3391, 3135, 2943, 2840, 1726, 1616, 1514, 1476 cm⁻¹. ¹H NMR (500 MHz, CDCl₃): 8.02 (d, *J* = 8.0 Hz, 1H, H₈), 7.92 (d, *J* = 8.0 Hz, 1H, H₅), 7.54 (t, *J* = 8.0 Hz, 1H, H₆), 7.45 (d, *J* = 9.0 Hz, 1H, H₅), 7.35 (t, *J* = 8.0 Hz, 1H, H₇), 7.32 (s, 1H, triazole), 6.80 (d, *J* = 9.0 Hz, 1H, H₆), 6.74 (s, 1H, H₈), 6.03 (s, 1H, H₃), 4.74 (s, 2H, NHCH₂), 4.33 (t, *J* = 6.0 Hz, 2H, CH₂), 3.97 (t, *J* = 6.0 Hz, 2H, CH₂), 3.04 (s, 2H, CH₂), 2.71 (t, 2H, CH₂), 2.36 (s, 2H, CH₃), 1.94–1.83 (m, 8H, 4 × CH₂), 1.46 (quin, *J* = 6.0 Hz, 2H, CH₂). ¹³C NMR (125 MHz, CDCl₃): 161.6, 161.1, 158.1, 155.2, 152.4, 150.2,

146.5, 145.6, 128.6, 128.0, 125.5, 124.2, 122.7, 121.2, 120.3, 117.5, 113.5, 112.4, 111.9, 101.3, 67.9, 50.0, 44.2, 33.5, 29.8, 28.2, 24.6, 22.9, 22.8, 22.5, 18.4. Anal. Calcd for C₃₁H₃₃N₅O₃: C, 71.11; H, 6.35; N, 13.37. Found: C, 71.27; H, 6.50; N, 13.53.

4.1.2.17. 7-((5-(4-(((6-Chloro-1,2,3,4-tetrahydroacridin-9-yl)amino)methyl)-1H-1,2,3-triazol-1-yl)pentyl)oxy)-4-methyl-2H-chromen-2-one (**8q**). Brown gum-solid; yield: 63%. IR (KBr): 3320, 3139, 2934, 2862, 1731, 1618, 1553, 1493 cm⁻¹. ¹H NMR (500 MHz, CDCl₃): 7.92 (d, *J* = 8.5 Hz, 1H, H₈), 7.86 (s, 1H, H₅), 7.43 (d, *J* = 9.0 Hz, 1H, H₅), 7.31 (s, 1H, triazole), 7.26 (d, *J* = 8.5 Hz, 1H, H₇), 6.79 (d, *J* = 8.5 Hz, 1H, H₆), 6.72 (s, 1H, H₈), 6.07 (s, 1H, H₃), 4.68 (s, 2H, NHCH₂), 4.33 (t, *J* = 6.0 Hz, 2H, CH₂), 3.96 (s, 2H, CH₂), 2.99 (s, 2H, CH₂), 2.69 (s, 2H, CH₂), 2.35 (s, 3H, CH₃), 1.93–1.84 (m, 8H, 2 × CH₂), 1.58 (s, 2H, CH₂). ¹³C NMR (125 MHz, CDCl₃): 161.8, 161.0, 159.9, 155.1, 152.4, 149.9, 147.8, 145.4, 133.9, 127.6, 125.4, 124.7, 124.3, 121.0, 118.9, 118.0, 113.4, 112.3, 111.7, 101.3, 67.8, 50.0, 44.3, 33.9, 29.8, 28.2, 24.5, 22.9, 22.7, 22.8, 18.2. Anal. Calcd for C₃₁H₃₂ClN₅O₃: C, 66.72; H, 5.78; N, 12.55. Found: C, 66.58; H, 5.60; N, 12.37.

4.1.2.18. 7-((5-(4-(((7-Chloro-1,2,3,4-tetrahydroacridin-9-yl)amino)methyl)-1H-1,2,3-triazol-1-yl)pentyl)oxy)-4-methyl-2H-chromen-2-one (**8r**). Brown gum-solid; yield: 59%. IR (KBr): 3341, 3129, 2933, 2845, 1724, 1617, 1559, 1491 cm⁻¹. ¹H NMR (500 MHz, CDCl₃): 7.96 (s, 1H, H₈), 7.82 (d, *J* = 8.5 Hz, 1H, H₅), 7.48–7.31 (m, 3H, H₅, H₆, triazole), 6.78 (dd, *J* = 8.0, 2.0 Hz, 1H, H₆), 6.74 (d, *J* = 2.0 Hz, 1H, H₈), 6.07 (s, 1H, H₃), 4.67 (s, 2H, NHCH₂), 4.37 (t, *J* = 6.0 Hz, 2H, CH₂), 3.96 (t, *J* = 6.0 Hz, 2H, CH₂), 3.00 (s, 2H, CH₂), 2.70 (s, 2H, CH₂), 2.34 (s, 3H, CH₃), 1.95 (quin, *J* = 6.0 Hz, 2H, CH₂), 1.83–1.82 (m, 8H, 4 × CH₂), 1.47 (quin, *J* = 6.0 Hz, 2H, CH₂). ¹³C NMR (125 MHz, CDCl₃): 161.7, 161.0, 158.5, 155.0, 152.3, 149.4, 145.3, 143.6, 129.7, 129.5, 129.1, 125.3, 121.7, 121.1, 120.1, 118.3, 113.3, 112.2, 111.6, 101.2, 67.8, 49.9, 44.0, 33.4, 29.7, 28.1, 24.6, 22.8, 22.6, 22.5, 18.6. C₃₁H₃₂ClN₅O₃: C, 66.72; H, 5.78; N, 12.55. Found: C, 66.56; H, 5.58; N, 12.39.

4.2. AChE and BChE inhibition assay

Acetylcholinesterase (AChE, E.C. 3.1.1.7, Type V-S, lyophilized powder, from electric eel), butylcholinesterase (BChE, E.C. 3.1.1.8, from equine serum), acetylthiocholine iodide (ATCI), butyrylthiocholine iodide (BTCI) and 5,5-dithiobis-(2-nitrobenzoic acid) (DTNB) were purchased from Sigma-Aldrich. Potassium dihydrogen phosphate, dipotassium hydrogen phosphate, potassium hydroxide, and sodium hydrogen carbonate were obtained from Fluka. The solutions of the title compounds were prepared in a mixture of DMSO (5 mL) and methanol (5 mL) and diluted in 0.1 M KH₂PO₄/K₂HPO₄ buffer (pH 8.0) to obtain final assay concentrations. All experiments were achieved at 25 °C. Four different concentrations were tested for each compound in triplicate to obtain the range of 20%–80% inhibition for AChE.

To measure *in vitro* AChE activity, modified Ellman's method [34,41] was performed using a 96-well plate reader (BioTek ELX808). Each well contained 50 μL potassium phosphate buffer (KH₂PO₄/K₂HPO₄, 0.1 M, pH 8), 25 μL sample dissolved in 50% methanol and 50% DMSO and 25 μL enzyme (final concentration 0.22 U/mL in buffer). They were preincubated for 15 min at room temperature, then 125 μL DTNB (3 mM in buffer) was added. Characterization of the hydrolysis of ATCI catalyzed by AChE was performed spectrometrically at 405 nm followed by the addition of substrate (ATCI 3 mM in water). The change in absorbance was measured at 405 nm after 20 min. The IC₅₀ values were determined graphically from inhibition curves (log inhibitor concentration vs. percent of inhibition). A control experiment was performed under the same conditions without inhibitor and the blank contained buffer, DMSO, DTNB, and substrate. The described method was also used for BChE inhibition assay.

4.3. Kinetic studies of AChE and BChE inhibition

For estimates of the inhibition model and inhibition constant K_i , reciprocal plots of $1/V$ versus $1/[S]$ were obtained using different concentrations of the substrate. For this purpose, experiments were performed similar to enzyme inhibition assay [34]. The rate of enzymatic reaction was obtained with different concentrations of inhibitor and in the absence of inhibitor. For each experiment, reaction was started by adding substrate and progress curves were recorded at 405 nm over 2 min. Next, double reciprocal plots ($1/v$ vs. $1/[s]$) were made using the slopes of progress curves to obtain the type of inhibition. Slopes of these reciprocal plots were then plotted against the concentration of compound in a weighted analysis, and K_i was determined as the intercept on the negative x-axis. All rate measurements were performed in triplicate and data analysis was performed with Microsoft Excel 2003.

4.4. BACE1 enzymatic assay

The BACE1 enzyme inhibition assay was carried out using a FRET (Forster resonance energy transfer) kit, from Invitrogen (former Pan Vera corporation, Madison, WI) according to the manufacturer instructions. BACE1 (purified baculovirus-expressed enzyme) was diluted with the assay buffer (50 mM sodium acetate, pH 4.5) to make a 3X working solution of 1 U/mL. The peptide substrate (Rh-EVNLDAEFK-Quencher) was also diluted with the same assay buffer to provide the 3× stock solution (750 nM). The inhibitor stock solutions in DMSO were diluted with buffer to provide 3× solution of test compounds at different concentrations. The 3× solution of BACE1 enzyme (10 mL) and each inhibitor sample (10 mL) were placed in 96-well plates and gently mixed. The substrate 3× solution (10 mL) was then added to this mixture in each well to start the reaction at the final reaction volume of 30 mL the final concentration of DMSO in each sample and control wells was equal or less than 6%. The reaction mixtures were incubated at 25 °C for 90 min in the dark and then the reaction was stopped by adding 10 mL of 2.5 mM sodium acetate. Fluorescence was monitored at 544 nm (excitation wave length) and 590 nm (emission wavelength). OM99-2 was used as a reference inhibitor compound. A multi-well spectrofluorometer instrument (BMG LABTECH, Polar star, Germany) was used for measurements. IC_{50} values were calculated with Curve Expert software version 1.34 for Windows. Each experiment was repeated for three to four times. All data were presented as mean \pm S.E.M.

4.5. Neuroprotection assay against $A\beta$ -induced damage

PC12 Cells were grown in monolayer culture on collagen-coated plates at 37 °C in humidified air containing 5% CO_2 . Two-thirds of the growth medium was changed every 3–4 days and the cells were sub-cultured once a week. Evaluation of compound **8e** for protecting neuronal PC12 cells against $A\beta_{25-35}$ induced damage was examined by the MTT assay [35]. Stock solution of $A\beta_{25-35}$ (0.5 mM) was prepared in distilled water and was diluted in media at a concentration of 55 μ M. PC12 cells at a density of 5×10^5 cells/ml (100 mL in each well) were seeded in rat-tail collagen-coated 96-well plates and incubated for 48 h to adhere at 37 °C. Compound **8e** at various concentrations was added in triplicate and incubated for 3 h. Human $A\beta_{25-35}$ was then added at a final concentration of 5 mM. After 24 h, 90 mL of the medium was taken out and 20 mL of MTT (0.5 mg/ml dissolved in RPMI containing phenol red) was added and incubated for an additional 2 h at 37 °C. Afterwards, formazan crystals were solubilized in 200 mL DMSO. The optical density was measured at 570 nm with background correction at 655 nm using a Bio-Rad microplate reader (Model 680, Bio-Rad). Each experiment was repeated 3–5 times. The percentage of protection was calculated: Protection of cells (%) = $[(A_0 - A_b)/(100 - A_b)] \times 100$. A_0 is the viability % of the cell in the presence of $A\beta$ and compound **8e**, $A\beta$ is

the viability % of cells in the presence of $A\beta$ regarded as 0% protection.

4.6. Molecular docking studies

Molecular docking studies were performed using the Autodock 4.2 program for the most potent anti-AChE compounds **8e**, **8h**, and **8q**. For this purpose, the crystal structure of torpedo californica acetylcholinesterase (2CKM) was retrieved from the Brookhaven protein database (<http://www.rcsb.org>). Subsequently, the water molecules and the original inhibitors were deleted from the protein structure. The 3D structure of the compounds was provided using MarvinSketch 5.8.3, 2012, ChemAxon (<http://www.chemaxon.com>) and converted to pdbqt coordinate by Autodock Tools (ADT; version 1.5.4). To obtain enzyme. pdbqt, polar hydrogen atoms were added to amino acid residues, Koulman charges were assigned to all atoms of the enzyme using Autodock Tools (ADT; version 1.5.4). All maps were calculated with 0.375 Å spacing between grid points by Autogrid. The center of the grid box was placed at the center of donepezil with coordinates $x = 3.771$, $y = 63.616$, $z = 63.737$. The dimensions of the active site box were set at $60 \times 60 \times 60$ Å. The docking was carried out with 100 runs using the Lamarckian genetic algorithm (LGA). Other parameters were accepted as default. A cluster analysis was performed on the docking results using a root mean square (RMS) tolerance of 2.0 and the lowest energy conformation of the highest populated cluster was selected for analysis. Graphic visualizations were done by Discovery Studio 4.0 client software.

Moreover, docking simulations for the most potent anti-BChE compounds **8a**, **8h**, and **8m** was carried out by Autodock Vina (AV) 1.1.1 program [36]. The crystal structure of human butyrylcholinesterase (4BDS) was retrieved from Protein Data Bank. Then, the water molecules and inhibitor were removed and enzyme. pdbqt was prepared by Autodock Tools (ver 1.5.4) with default parameters. The selected compounds and their 3D structure were generated by MarvinSketch 5.8.3, 2012 and then ligand.pdbqt was provided by Autodock Tools (ver 1.5.4). The Autodock Vina parameters were set as follow; box size: $60 \times 60 \times 60$ Å, the center of box: $x = 135.943$, $y = 112.748$, $z = 40.693$ (geometrical center of co-crystallized ligand), the exhaustiveness: 10 and the other parameters were left unchanged. The calculated geometries were ranked in terms of free energy of binding and the best pose was selected for further analysis. Molecular visualizations were performed by Discovery Studio 4.0 client software (Accelrys, Inc., San Diego, CA).

4.7. Learning and memory evaluation by Morris water maze test (MWM)

4.7.1. Drugs

All drugs including scopolamine hydrobromide and donepezil hydrochloride were obtained from Sigma. They were dissolved in saline and the test compound **8e** was dissolved in 20% PEG 400 (Polyethylene glycol) as drug vehicle.

4.7.2. Animals

Male albino Wistar rats (200–220 g) were obtained from the Faculty of Pharmacy, Tehran University of Medical Sciences. They were randomly selected to experimental groups. A 12-hrs light/12-hrs dark cycle was kept and provided food and water ad libitum. The room was maintained at the temperature 25 ± 2 °C. Our experiments were in agreement with the guidelines of “Institutional Guide for the Care and Use of Laboratory Animals” and were approved by the Ethical Committee for the Care and Use of Laboratory Animals at Tehran University of Medical Sciences.

4.7.3. Morris water maze test

Rats were trained for 4 successive days in a Morris water maze (MWM) apparatus which was a black circular pool with a diameter of

about 136 cm and a depth of 35 cm. The pool was filled with water and the temperature was kept at 25 ± 2 °C. Walls were covered by different shaped visual cues. A circular-shaped invisible platform made of Plexiglass whose diameter is 10 cm was submersed 1 cm below the water surface in the northwest quadrant of the pool (target quadrant). In each trial, rats were randomly released into the water at starting point of a pool quadrant. A camera was installed above the pool and connected to a computer equipped with Ethovision software (Noldus Information Technology, Wageningen, Netherlands) to record the swimming pathway and obtain the related data. Rats were allowed to swim freely maximum for 90 s. If rats did not find the platform during this period of time, they were manually conducted to the platform. Then, they were allowed to stay on the platform for 20 s. On the first 4 day, the rats were given daily sessions of 4 trials lasted for 90 s. At this step, quantitative data was provided in terms of escape latency, traveled distance, swimming speed for first 4 days of training and time spent in the target quadrant (Q_1) on fifth day (probe trial test). It should be noted that the platform in the target quadrant was removed and animals did not receive treatment on test day. However, they were treated for 4 days of training.

4.7.4. *In vivo drug treatment*

In this study, eleven groups of rats were investigated. All drugs were administrated by intraperitoneal injection (IP). The escape latency, traveled distance, swimming speed for first 4 days of trial (training days) and time spent in target quadrant fifth day of trial (probe trial test) were evaluated for all groups.

4.7.4.1. Control group. The control group was given normal saline (5 mg/kg) 30 min prior to testing.

4.7.4.2. Scopolamine group. Scopolamine hydrobromide (4 mg/kg) was administered 30 min before each trial for first 4 days of trials.

4.7.4.3. Vehicle group. 20% PEG 400 (5 mL/kg) was administered to rats 30 min before subjecting to the first 4 days of trials.

4.7.4.4. The compound **8e groups (0.3, 0.6, 1.25, 2.5, 5, and 10 mg/kg).** The most potent AChEI activity compound (**8e**) and scopolamine (4 mg/kg) were administered to rats 60 min and 30 min before subjecting to the first 4 days of trials, respectively.

4.7.4.5. Donepezil group (1.25, 2.5 mg/kg). Donepezil and scopolamine (4 mg/kg) were administered to rats 60 min and 30 min before subjecting to the first 4 days of trials, respectively.

4.7.5. Statistical analysis

One-way analysis of variance (ANOVA) followed by Bonferroni and Newman-Keuls multiple comparison tests were used for the comparison of test groups, first 4 days of trials (training days), and post training probe trial test, respectively.

Acknowledgments

This work was supported by grants from the Research Council of Tehran University of Medical Sciences with project No. 94-01-33-28713.

Conflict of interest

All authors declare no conflict of interest.

References

- [1] M. Goedert, M.G. Spillantini, A century of Alzheimer's disease, *Science* 314 (2006) 777–781.
- [2] C. Ballard, S. Gauthier, A. Corbett, C. Brayne, D. Aarsland, E. Jones, Alzheimer's disease, *Lancet* 377 (2011) 1019–1031.
- [3] X. Zhu, H.G. Lee, G. Perry, M. Smith, Alzheimer disease, the two-hit hypothesis: an update, *Biochim. Biophys. Acta* 1772 (2007) 494–502.
- [4] R.J. Caselli, T.G. Beach, D.S. Knopman, N.R. Graff-Radford, Alzheimer disease: scientific breakthroughs and translational challenges, *Mayo Clin. Proc.* 92 (2017) 978–994.
- [5] X. Zhang, K.P. Rakesh, S.N.A. Bukhari, M. Balakrishna, H.M. Manukumar, H.L. Qin, Multi-targetable chalcone analogs to treat deadly Alzheimer's disease: current view and upcoming advice, *Bioorg. Chem.* 80 (2018) 86–93.
- [6] G.S. Bloom, Amyloid- β and tau: the trigger and bullet in Alzheimer disease pathogenesis, *JAMA Neurol.* 71 (2014) 505–508.
- [7] M. Jouanne, S. Rault, A.S. Voisin-Chiret, Tau protein aggregation in Alzheimer's disease: an attractive target for the development of novel therapeutic agents, *Eur. J. Med. Chem.* 139 (2017) 153–167.
- [8] W.J. Huang, X. Zhang, W.W. Chen, Role of oxidative stress in Alzheimer's disease, *Biomed. Rep.* 4 (2016) 519–522.
- [9] P. Zatta, D. Drago, S. Bolognin, S.L. Sensi, Alzheimer's disease, metal ions and metal homeostatic therapy, *Trends Pharmacol. Sci.* 7 (2009) 346–355.
- [10] M.T. Heneka, M.K. O'Banion, D. Terwel, M.P. Kummer, Neuroinflammatory processes in Alzheimer's disease, *J. Neural. Transm.* 117 (2010) 919–947.
- [11] A. Contestabile, The history of the cholinergic hypothesis, *Behav. Brain Res.* 221 (2011) 334–340.
- [12] N.H. Greig, T. Utsuki, Q. Yu, X. Zhu, H.W. Holloway, T. Perry, B. Lee, D.K. Ingram, D.K. Lahiri, A new therapeutic target in Alzheimer's disease treatment: attention to butyrylcholinesterase, *Curr. Med. Res. Opin.* 17 (2001) 159–165.
- [13] R.M. Lane, S.G. Potkin, A. Enz, Targeting acetylcholinesterase and butyrylcholinesterase in dementia, *Int. J. Neuropsychopharmacol.* 9 (2006) 101–124.
- [14] Y. Nicolet, O. Lockridge, P. Masson, J.C. Fontecilla-Camps, F. Nachon, Crystal structure of human butyrylcholinesterase and of its complexes with substrate and products, *J. Biol. Chem.* 278 (2003) 41141–41147.
- [15] H. Dvir, I. Silman, M. Harel, T.L. Rosenberry, J.L. Sussmana, Acetylcholinesterase: from 3D structure to function, *Chem. Biol. Interact.* 187 (2010) 10–22.
- [16] N.C. Inestrosa, A. Alvarez, C.A. Pérez, R.D. Moreno, M. Vicente, C. Linker, O.I. Casanueva, C. Soto, J. Garrido, Acetylcholinesterase accelerates assembly of amyloid-beta-peptides into Alzheimer's fibrils: possible role of the peripheral site of the enzyme, *Neuron* 16 (1996) 881–891.
- [17] M. Bartolini, C. Bertucci, V. Cavrini, V. Andrisano, beta-Amyloid aggregation induced by human acetylcholinesterase: inhibition studies, *Biochem. Pharmacol.* 65 (2003) 407–416.
- [18] G.A. Reid, S. Darvesh, Butyrylcholinesterase-knockout reduces brain deposition of fibrillar β -amyloid in an Alzheimer mouse model, *Neuroscience* 298 (2015) 424–435.
- [19] P. Anand, B. Singh, N. Singh, A review on coumarins as acetylcholinesterase inhibitors for Alzheimer's disease, *Bioorg. Med. Chem.* 20 (2012) 1175–1180.
- [20] L.G. de Souza, M.N. Rennä, J.D. Figueroa-Villar, Coumarins as cholinesterase inhibitors: a review, *Chem. Biol. Interact.* 254 (2016) 11–23.
- [21] S.S. Xie, J.S. Lan, X.B. Wang, N. Jiang, G. Dong, Z.R. Li, K.D. Wang, P.P. Guo, L.Y. Kong, Multifunctional tacrine-trolox hybrids for the treatment of Alzheimer's disease with cholinergic, antioxidant, neuroprotective and hepatoprotective properties, *Eur. J. Med. Chem.* 93 (2015) 42–50.
- [22] S.Y. Li, X.B. Wang, S.S. Xie, N. Jiang, K.D. Wang, H.Q. Yao, H.B. Sun, L.Y. Kong, Multifunctional tacrine-flavonoid hybrids with cholinergic, β -amyloid-reducing, and metal chelating properties for the treatment of Alzheimer's disease, *Eur. J. Med. Chem.* 69 (2013) 632–646.
- [23] Z. Najafi, M. Mahdavi, M. Saeedi, R. Sabourian, M. Khanavi, M. Safavi, M. Barazandeh Tehrani, A. Shafiee, A. Foroumadi, T. Akbarzadeh, 1,2,3-Triazole-isoxazole based acetylcholinesterase inhibitors: synthesis, biological evaluation and docking study, *Lett. Drug Des. Discov.* 14 (2017) 58–65.
- [24] Z. Najafi, M. Mahdavi, M. Saeedi, E. Karimpour-Razkenari, R. Asatouri, F. Vafadarnejad, F.H. Moghadam, M. Khanavi, M. Sharifzadeh, T. Akbarzadeh, Novel tacrine-1,2,3-triazole hybrids: *In vitro*, *in vivo* biological evaluation and docking study of cholinesterase inhibitors, *Eur. J. Med. Chem.* 125 (2017) 1200–1212.
- [25] M.K. Hu, C.F. Lu, A facile synthesis of bis-tacrine isosteres, *Tetrahedron Lett.* 41 (2000) 1815–1818.
- [26] W. Osman, T. Mohamed, V.M. Sit, M.S. Vasefi, M.A. Beazely, P.P. Rao, Structure-activity relationship studies of benzyl-, phenethyl-, and pyridyl-substituted tetrahydroacridin-9-amines as multitargeting agents to treat Alzheimer's disease, *Chem. Biol. Drug Des.* 88 (2016) 710–723.
- [27] F. Mao, J. Li, H. Wei, L. Huang, X. Li, Tacrine-propargylamine derivatives with improved acetylcholinesterase inhibitory activity and lower hepatotoxicity as a potential lead compound for the treatment of Alzheimer's disease, *J. Enzyme Inhib. Med. Chem.* 30 (2015) 995–1001.
- [28] H.V. Pechmann, Neue bildungsweise der cumarine. Synthese des daphnetins, *Ber. Dtsch. Chem. Ges.* 17 (1984) 929–936.
- [29] S.S. Xie, X. Wang, N. Jiang, W. Yu, K.D. Wang, J.S. Lan, Z.R. Li, L.Y. Kong, Multi-target tacrine-coumarin hybrids: cholinesterase and monoamine oxidase B inhibition properties against Alzheimer's disease, *Eur. J. Med. Chem.* 5 (2015) 153–165.
- [30] Y. Chen, S. Wang, X. Xu, X. Liu, M. Yu, S. Zhao, S. Liu, Y. Qiu, T. Zhang, B.F. Liu, G. Zhang, Synthesis and biological investigation of coumarin piperazine (piperidine) derivatives as potential multireceptor atypical antipsychotics, *J. Med. Chem.* 56 (2013) 4671–4690.
- [31] N. Jiang, Q. Huang, J. Liu, N. Liang, Q. Li, Q. Li, S.S. Xie, Design, synthesis and biological evaluation of new coumarin-dithiocarbamate hybrids as multifunctional agents for the treatment of Alzheimer's disease, *Eur. J. Med. Chem.* 146 (2018)

- 287–298.
- [32] K. Kushwaha, N. Kaushik, Lata, S.C. Jain, Design and synthesis of novel 2*H*-chromen-2-one derivatives bearing 1,2,3-triazole moiety as lead antimicrobials, *Bioorg. Med. Chem. Lett.* 24 (2014) 1795–1801.
- [33] H. Yu, Z. Hou, Y. Tian, Y. Mou, C. Guo, Design, synthesis, cytotoxicity and mechanism of novel dihydroartemisinin-coumarin hybrids as potential anti-cancer agents, *Eur. J. Med. Chem.* 10 (2018) 434–449.
- [34] G.L. Ellman, K.D. Courtney, V. Andres Jr, R.M. Feather-Stone, A new and rapid colorimetric determination of acetylcholinesterase activity, *Biochem. Pharmacol.* 7 (1961) 88–95.
- [35] A. Iraj, O. Firuzi, M. Khoshneviszadeh, M. Tavakkoli, M. Mahdavi, H. Nadri, N. Edraki, R. Miri, Multifunctional iminochromene-2*H*-carboxamide derivatives containing different aminomethylene triazole with BACE1 inhibitory, neuroprotective and metal chelating properties targeting Alzheimer's disease, *Eur. J. Med. Chem.* 141 (2017) 690–702.
- [36] O. Trott, A.J. Olson, AutoDock Vina: improving the speed and accuracy of docking with a new scoring function, efficient optimization and multithreading, *J. Comput. Chem.* 31 (2010) 455–461.
- [37] E.H. Rydberg, B. Brumshtein, H.M. Greenblatt, D.M. Wong, D. Shaya, L.D. Williams, P.R. Carlier, Y.P. Pang, I. Silman, J.L. Sussman, Complexes of alkylene-linked tacrine dimers with Torpedo californica acetylcholinesterase: binding of bis5-tacrine produces a dramatic rearrangement in the active-site gorge, *J. Med. Chem.* 49 (2006) 5491–5500.
- [38] F. Nachon, E. Carletti, C. Ronco, M. Trovaslet, Y. Nicolet, L. Jean, P. Renard, Crystal structures of human cholinesterases in complex with huprine W and tacrine: elements of specificity for anti-Alzheimer's drugs targeting acetyl- and butyrylcholinesterase, *Biochem. J.* 453 (2013) 393–399.
- [39] R. Morris, Developments of a water-maze procedure for studying spatial learning in the rat, *J. Neurosci. Methods.* 11 (1984) 47–60.
- [40] F. Asadi, A.H. Jamshidi, F. Khodaghali, A. Yans, L. Azimi, M. Faizi, L. Vali, M. Abdollahi, M.H. Ghahremani, M. Sharifzadeh, Reversal effects of crocin on amyloid β -induced memory deficit: modification of autophagy or apoptosis markers, *Pharmacol. Biochem. Behav.* 139 (2015) 47–58.
- [41] S. Arab, S.E. Sadat-Ebrahimi, M. Mohammadi-Khanaposhtani, A. Moradi, H. Nadri, M. Mahdavi, S. Moghimi, M. Asadi, L. Firoozpour, M. Pirali-Hamedani, A. Shafiee, A. Foroumadi, Synthesis and evaluation of chroman-4-one linked to *N*-benzyl pyridinium derivatives as new acetylcholinesterase inhibitors, *Arch. Pharm. Chem. Life Sci.* 348 (2015) 643–649.